A Study on High Precision Navigation Satellite System

Falin Wu

Supervisors: Akio Yasuda

Masaki Oshima

Laboratory of Communication Engineering

Tokyo University of Marine Science and Technology

Contents

1.1 Background

- Global Positioning System (GPS)
- Russian GLONASS
- European Galileo System
- Satellite Based Augmentation System (SBAS)
  - U.S.: Wide Area Augmentation System (WAAS)
  - Europe: European Geostationary Navigation Overlay System (EGNOS)
  - Japan: MTSAT Satellite Augmentation System (MSAS)
  - India: GPS And GEO Augmented Navigation (GAGAN)
  - Japanese Quasi-Zenith Satellite System (QZSS)
- Performance of the Future GNSS?

1.3 Research Objectives

- To Investigate Carrier Phase Based Positioning with the Current GPS
  - Develop an algorithm for GPS carrier phase ambiguity resolution with altitude-aiding
  - Estimate the distance-dependant delays using MRS
- To Evaluate the Performance of High Precision Positioning with the Future GNSS
  - Evaluate the performance of hybrid modernized GPS and Galileo
  - Analyze the performance of GPS augmentation using QZSS
  - Develop a prototype software GPS receiver

2. GPS Carrier Phase Based Positioning

To Investigate Carrier Phase Based Positioning with the Current GPS

- Observation Models and Their Linear Combinations
  - Double Difference
  - Linear Combinations of Observables
- Ambiguity Resolution with Altitude-aiding
  - Ambiguity resolution approach
  - Numerical Results
- Estimation of Ionospheric Delays Using MRS
  - Ionospheric Correction Modelling
  - Numerical Results

2.2.1 GPS Observable Models

- Double Difference

$$
\begin{aligned}
\nabla\triangle P_1 &= \nabla\triangle\rho + \nabla\triangle I + \nabla\triangle T + \nabla\triangle M_{P_1} + \nabla\triangle e_1 \\
\nabla\triangle P_2 &= \nabla\triangle\rho + \left(\frac{f_1}{f_2}\right)^2 \nabla\triangle I + \nabla\triangle T + \nabla\triangle M_{P_2} + \nabla\triangle e_2 \\
\nabla\triangle \Phi_1 &= \nabla\triangle\rho - \nabla\triangle I + \nabla\triangle T + \nabla\triangle M_{\Phi_1} \\
&\quad + \lambda_1 \nabla\triangle N_1 + \nabla\triangle \varepsilon_1 \\
\nabla\triangle \Phi_2 &= \nabla\triangle\rho - \left(\frac{f_1}{f_2}\right)^2 \nabla\triangle I + \nabla\triangle T + \nabla\triangle M_{\Phi_2} \\
&\quad + \lambda_2 \nabla\triangle N_2 + \nabla\triangle \varepsilon_2
\end{aligned}
$$

2.2.1 Linear Combinations

- Widelane and Narrowlane Combinations

$$
\begin{aligned}
\nabla\triangle\Phi_W &= \nabla\triangle\rho + \frac{\lambda_2}{\lambda_1}\nabla\triangle I + \nabla\triangle T + \nabla\triangle M_{\Phi_W} \\
&\quad +\lambda_W\nabla\triangle N_W + \nabla\triangle\varepsilon_W \\
\nabla\triangle\Phi_N &= \nabla\triangle\rho - (\frac{\lambda_2}{\lambda_1})\nabla\triangle I + \nabla\triangle T + \nabla\triangle M_{\Phi_N} \\
&\quad +\lambda_N\nabla\triangle N_N + \nabla\triangle\varepsilon_N \\
\nabla\triangle N_W &= \nabla\triangle N_1 - \nabla\triangle N_2 \\
\nabla\triangle N_N &= \nabla\triangle N_1 + \nabla\triangle N_2 \\
\lambda_W &= \frac{\lambda_1\lambda_2}{\lambda_2 - \lambda_1} \approx 86.2cm \\
\lambda_N &= \frac{\lambda_1\lambda_2}{\lambda_2 + \lambda_1} \approx 10.7cm
\end{aligned}
$$

2.2.1 Linear Combinations

- Ionospheric-free Combination

$$\begin{aligned}\nabla\triangle\Phi_{IF} &= \frac{\nabla\triangle\Phi_W + \nabla\triangle\Phi_N}{2} \\ &= \nabla\triangle\rho + \frac{\lambda_N\nabla\triangle N_N + \lambda_W\nabla\triangle N_W}{2} + \nabla\triangle T \\ &\quad +\nabla\triangle M_{\Phi_{IF}} + \nabla\triangle\varepsilon_{IF}\end{aligned}$$

- Ionospheric-signal Combination

$$\begin{aligned}\nabla\triangle\Phi_{IS} &= \nabla\triangle\Phi_N - \nabla\triangle\Phi_W \\ &= -2\frac{\lambda_2}{\lambda_1}\nabla\triangle I + \lambda_N\nabla\triangle N_N - \lambda_W\nabla\triangle N_W \\ &\quad +(\nabla\triangle M_{\Phi_N} - \nabla\triangle M_{\Phi_W}) + (\nabla\triangle\varepsilon_N - \nabla\triangle\varepsilon_W)\end{aligned}$$

2.2.1 Linear Combinations

- Ionosphere Combination

$$
\begin{aligned}
\nabla\Delta\Phi_{ion} &= \nabla\Delta\Phi_1 - \nabla\Delta\Phi_2 \\
&= \lambda_1\nabla\Delta N_1 - \lambda_2\nabla\Delta N_2 + \left[\left(\frac{f_1}{f_2}\right)^2 - 1\right]\nabla\Delta I \\
&\quad +\varepsilon_{\nabla\Delta\Phi_{ion}} \\
&= \frac{\lambda_1}{60}\left(60\nabla\Delta N_1 - 77\nabla\Delta N_2\right) + \left[\left(\frac{f_1}{f_2}\right)^2 - 1\right]\nabla\Delta I \\
&\quad +\varepsilon_{\nabla\Delta\Phi_{ion}} \\
&= \frac{\lambda_1}{60}\nabla\Delta N_{ion} + \left[\left(\frac{f_1}{f_2}\right)^2 - 1\right]\nabla\Delta I + \varepsilon_{\nabla\Delta\Phi_{ion}}
\end{aligned}
$$

2.3.1 Ambiguity Resolution Approach

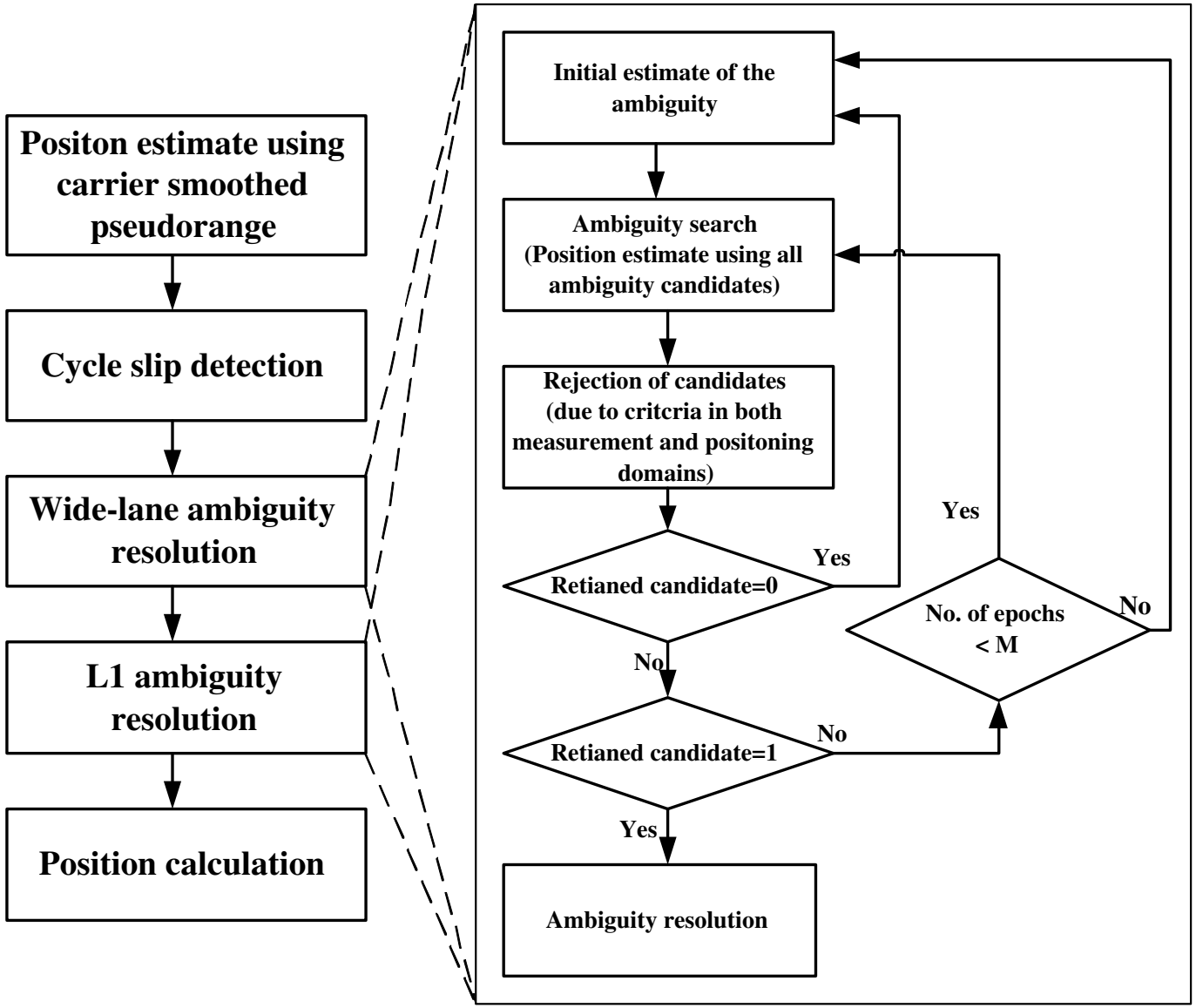

2.3.1.1 Cycle Slip Detection

- Time Difference of the Ionospheric-signal Combination

$$
\begin{aligned}
\delta\Phi_{IS} &= \nabla\triangle\Phi_{IS}(t_n) - \nabla\triangle\Phi_{IS}(t_{n-1}) \\
&= -\frac{2\lambda_2}{\lambda_1}\left[\nabla\triangle I(t_n) - \nabla\triangle I(t_{n-1})\right] \\
&\quad +(\lambda_N - \lambda_W)\delta N_1 + (\lambda_N + \lambda_W)\delta N_2 \\
&\approx -\frac{2\lambda_2}{\lambda_1}\left[\nabla\triangle I(t_n) - \nabla\triangle I(t_{n-1})\right] \\
&\quad +75.5 \cdot \delta N_1 + 96.9 \cdot \delta N_2 \ (cm)
\end{aligned}
$$

- Cycle Slip
  If $\delta\Phi_{IS} \geq$ a threshold value.

2.3.1.2 Wide-lane Ambiguity Resolution

- Procedure 1: Define Search Grid
  - $\nabla\triangle N_W = \left[\frac{\nabla\triangle\Phi_W - \nabla\triangle\rho - \nabla\triangle T}{\lambda_W}\right]_{roundoff}$
  - $\hat{N}_W^i - k\sigma_N^W \leq N_W^i \leq \hat{N}_W^i + k\sigma_N^W$
    $\sigma_N^W = \sqrt{(\sigma_m^{PR})^2 + (\sigma_m^W)^2} = \sqrt{65^2 + 4^2} \approx 65.12\,(cm)$
- Procedure 2: Ambiguity Search
  - Candidate rejection using altitude-aiding
    $(A^W > A_{max}) \bigcup (A^W < A_{min})$
  - Test in measurement domain: $\frac{\nu^T C_W^{-1} \nu}{df} > \frac{\chi^2_{df,1-\alpha}}{df} \cdot k_1^W$
  - Test in positioning domain: $|r^{PR} - r^W|_H > k_2^W \sigma_H^{PR-W}$
    $\sigma_H^{PR-W} = RHDOP \cdot \sigma_N^W \approx 65.12 \cdot RHDOP\,(cm)$
- Procedure 3: Determine Ambiguities

2.3.1.2.2.1 Altitude-aiding

- Altitude-aiding (A_{min}, A_{max})
  - Water Level Information
  - GIS
  - Other Information
- Water Level Information

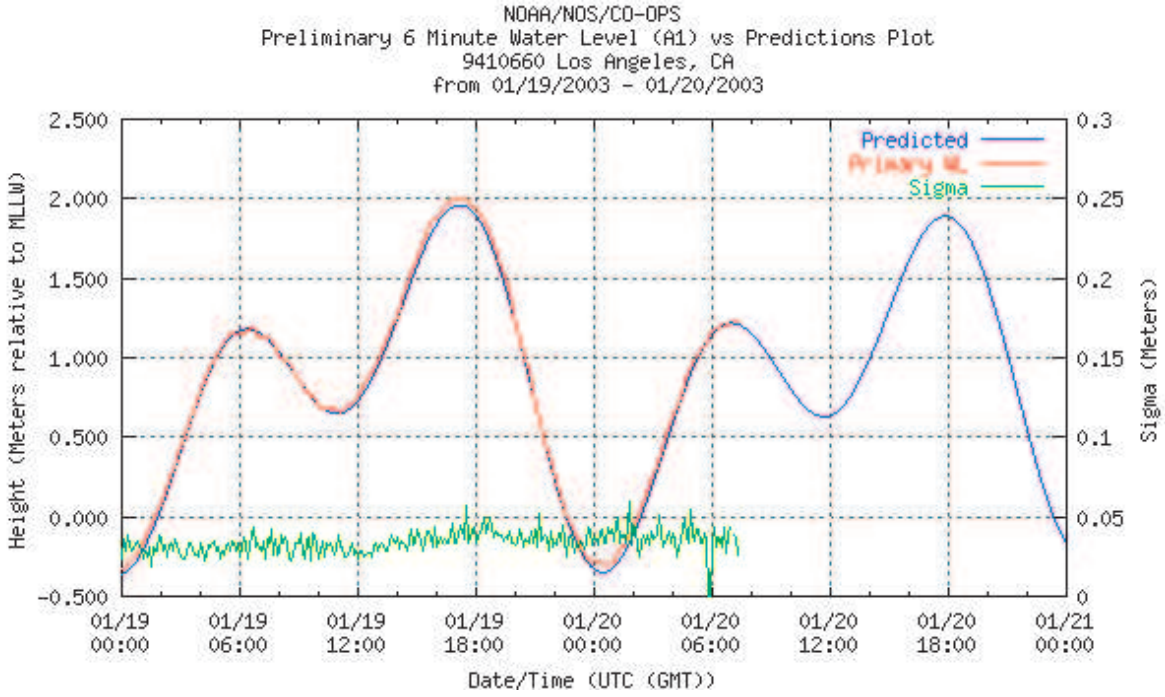

2.3.2 Experiment

- Experiment (July 9, 2002, Tokyo Bay):
  - *Marine-RTK*: Altitude-aiding method
  - *Marine-VRS*: VRS method

1) Reference Station
   - *Marine-RTK*: TUMST
   - *Marine-VRS*: Adachi, Yokohama and Ichihara
2) Baseline Length: 3.5 km
3) Four Bridges

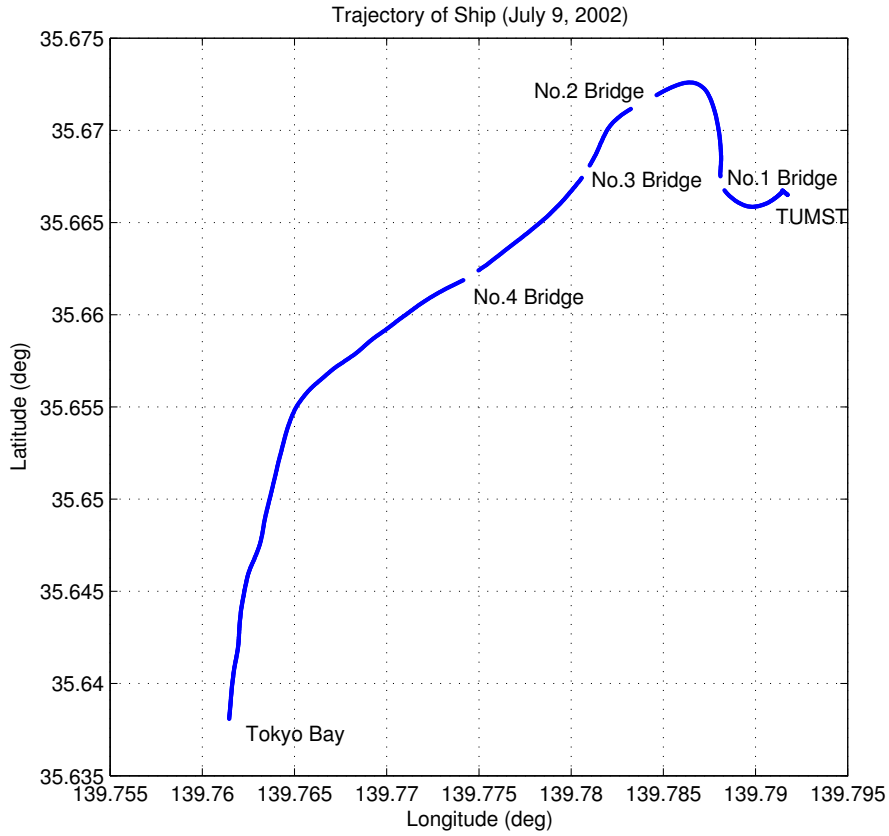

2.3.2.2 Altitude-aiding

- Altitude-aiding: *Marine-VRS*'s result
- Altitude variations of ship when it sailed from *TUMST* to *Rainbow Bridge*: $A_{min} = 39.8$ m and $A_{max} = 41.2$ m.

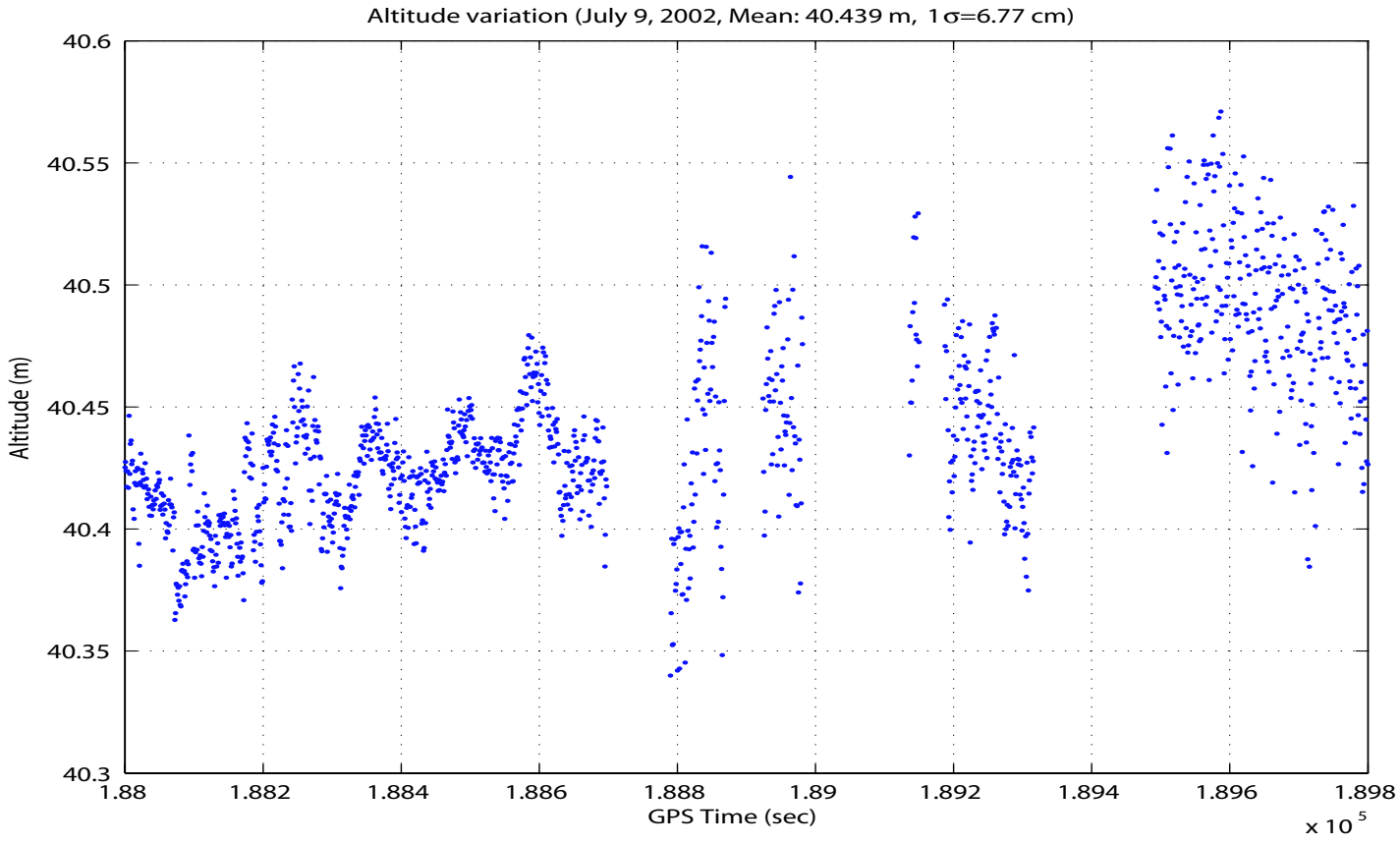

2.3.2.2.2 Altitude Variations (4 bridges)

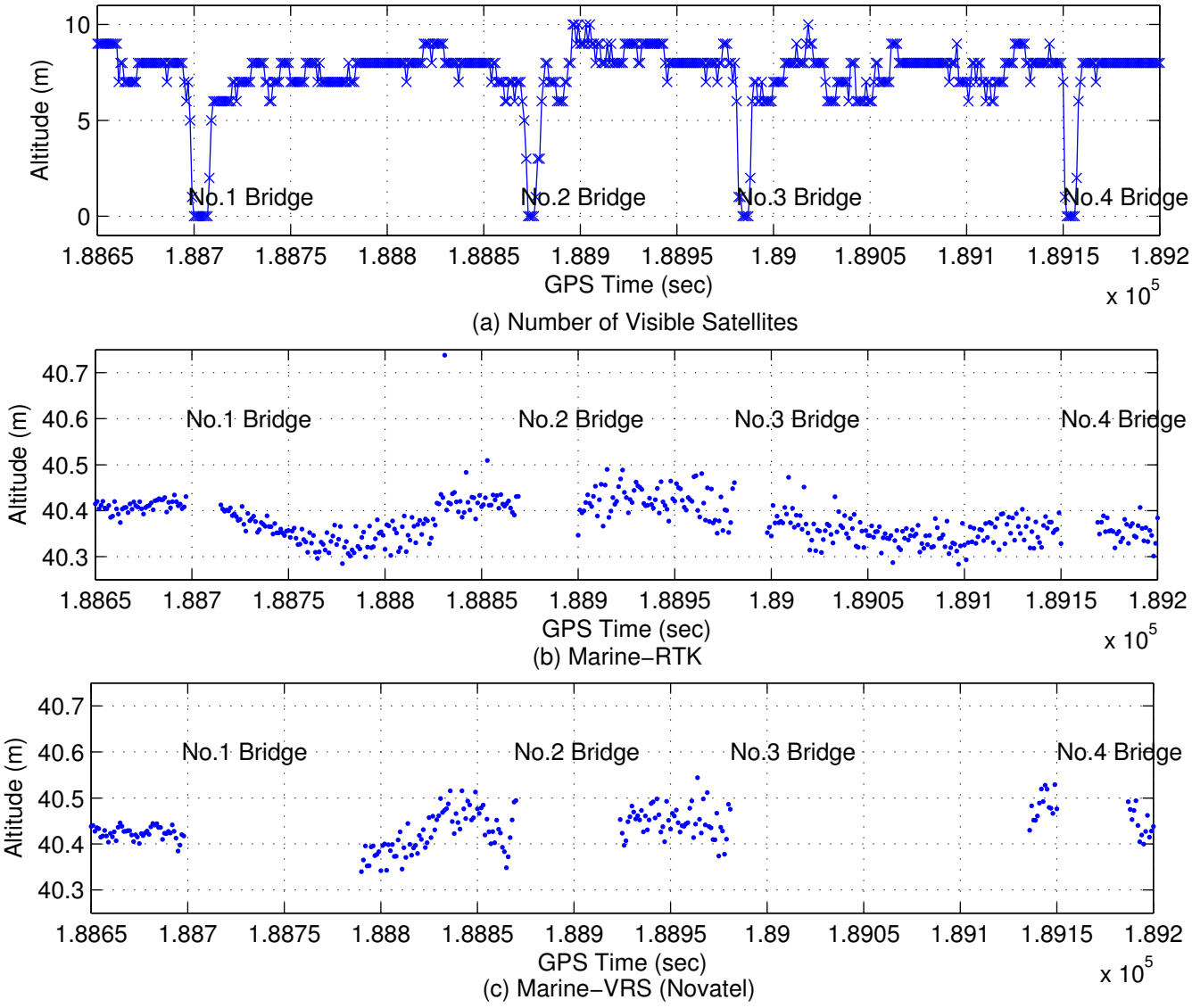

2.3.2.2.2 Performances

- Time to Fixed (sec)

Bridges		No.1	No.2	No.3	No.4
Marine-RTK	With Altitude-aiding	1	6	1	1
	Without Altitude-aiding	11	11	24	1
Marine-VRS	Novatel	75	35	138	18
	Astech	33	16	18	20
	Leica	19	32	23	18

- Fixed Percentages

		Fixed Percentage
Marine-RTK	With Altitude-aiding	97.5%
	Without Altitude-aiding	95.3%
Marine-VRS	Novatel	81.2%
	Astech	90.6%
	Leica	92.1%

2. GPS Carrier Phase Based Positioning

- Observation Models and Linear Combinations
  - Double Difference
  - Linear Combinations of Observables
- Ambiguity Resolution with Altitude-aiding
  - Ambiguity resolution approach
  - Numerical Results
- ***Estimation of Ionospheric Delays Using MRS***
  - Introduction
  - Ionospheric Correction Modelling
  - Numerical Results

2.4.1 Introduction

- GSI: GPS Earth Observation NETwork (GEONET)
  - 1,200 GPS based control stations
  - Baseline length: 50 km
  - Data Rate: $\frac{1}{30}$ Hz

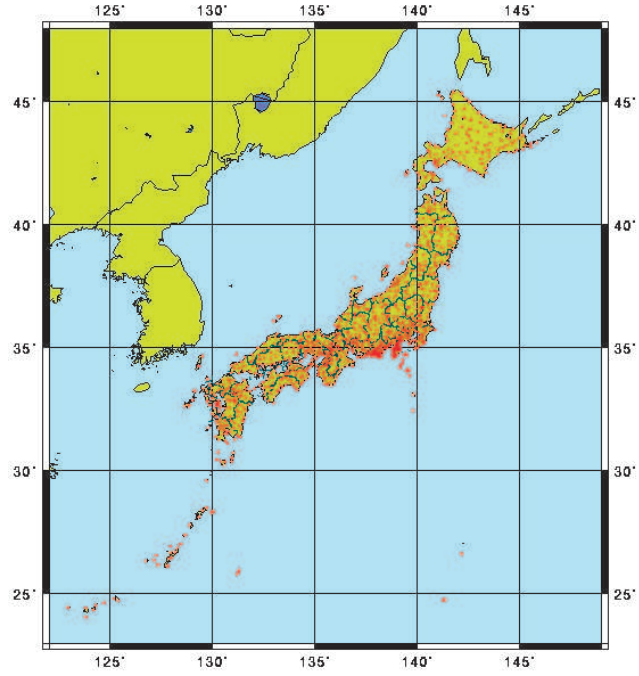

- Estimate the Ionospheric Delays Using GEONET.
  Data Rate: $\frac{1}{30}$ Hz $\rightarrow$ 1 Hz
  - Interpolation: Post-processing
  - Extrapolation: Real-time applications

2.4.2 Ionospheric Correction Modelling

1. Interpolation and Extrapolation of GEONET Reference Stations Data (Lagrange Interpolating Polynomial)

$$P(x) = \sum_{k=0}^{n} f(x_k) L_{n,k}(x), \text{ where } L_{n,k}(x) = \prod_{\substack{i=0 \\ i \neq k}}^{n} \frac{x - x_i}{x_k - x_i}$$

2. Ambiguity Resolution for Reference Stations

3. Ionospheric Delays Interpolation for Rover Station

$$\nabla\Delta\hat{I} = \frac{\nabla\Delta\Phi_1 + \lambda_1\nabla\Delta N_1 - (\nabla\Delta\Phi_2 - \lambda_2\nabla\Delta N_2)}{\left[\left(\frac{f_1}{f_2}\right)^2 - 1\right]}$$

$$\nabla\Delta\hat{I}_u = \sum_{i=1}^{n-1} \frac{w_{i,n}}{w} \nabla\Delta\hat{I}_{i,n}, \text{ with } w = \sum_{i=1}^{n-1} w_{i,n}, \; w_{i,n} = \frac{1}{d_{i,n}}$$

4. Estimated Ionospheric Delays Are Used to Reduce Ionospheric Delays at the Rover Station

2.4.2.2 Ambiguity Resolution Procedure

1. Define Ambiguities Search Space

$$\nabla\Delta N^0_{ion} = \left[\frac{60\nabla\Delta\Phi_{ion}}{\lambda_1}\right]_{roundoff}$$

$$\left|\nabla\Delta N_{ion} - \nabla\Delta N^0_{ion}\right| \leq c \cdot \frac{\lambda_1}{60}\sigma_{\nabla\Delta\Phi_{ion}}$$

2. Determine the Integer Ambiguities

- $\nabla\Delta\hat{I} = \dfrac{\nabla\Delta\Phi_{ion} - \frac{\lambda_1}{60}\nabla\Delta N_{ion}}{\left[\left(\frac{f_1}{f_2}\right)^2 - 1\right]}$
- $\nabla\Delta\hat{N}_W = \dfrac{\nabla\Delta\Phi_W - \nabla\Delta\rho - \frac{f_1}{f_2}\nabla\Delta\hat{I} - \nabla\Delta T}{\lambda_W}$
- $\nabla\Delta\hat{N}_1 = \dfrac{77\nabla\Delta\hat{N}_W - \nabla\Delta N_{ion}}{17}$, $\nabla\Delta\hat{N}_2 = \dfrac{60\nabla\Delta\hat{N}_W - \nabla\Delta N_{ion}}{17}$
- $\frac{r_2}{r_1} > C_{threshold}$, where r wide-lane residue

3. Ambiguity Confirmation

2.4.3.1 Test

- July 5, 2002, Konto area, Japan;
  - Master: SHIB (1 Hz)
  - Secondary (GEONET): ($\frac{1}{30}$ Hz $\rightarrow$ 1 Hz) R0584, R3027, R3019
  - Rover: USER (1 Hz)

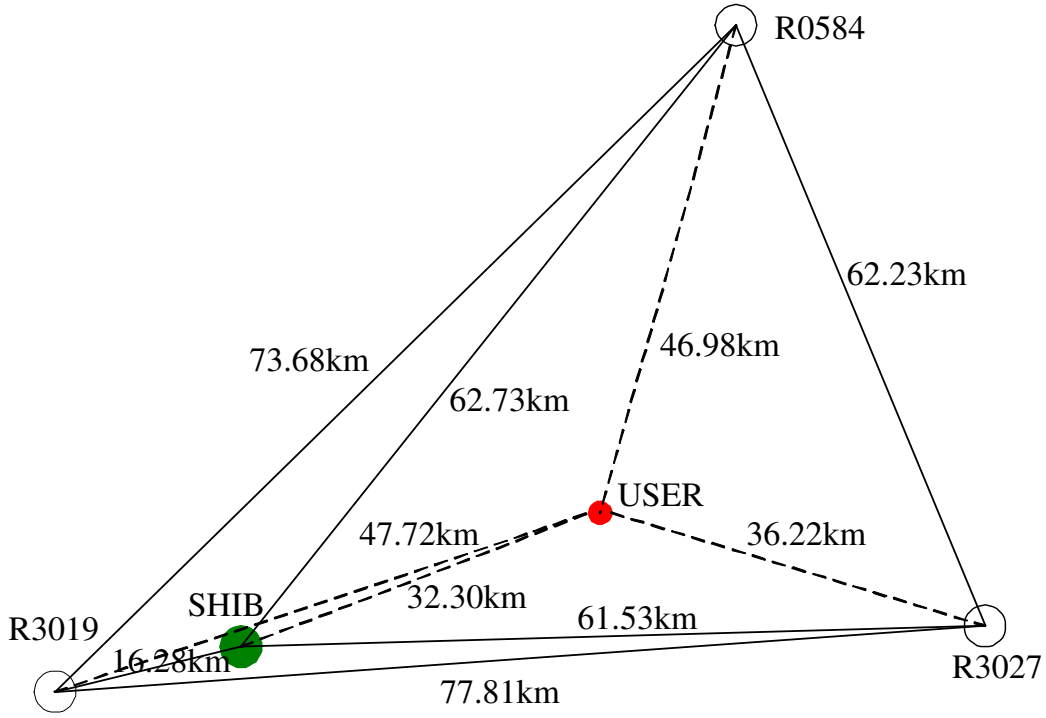

2.4.3.3 Ionosphere Correction Errors

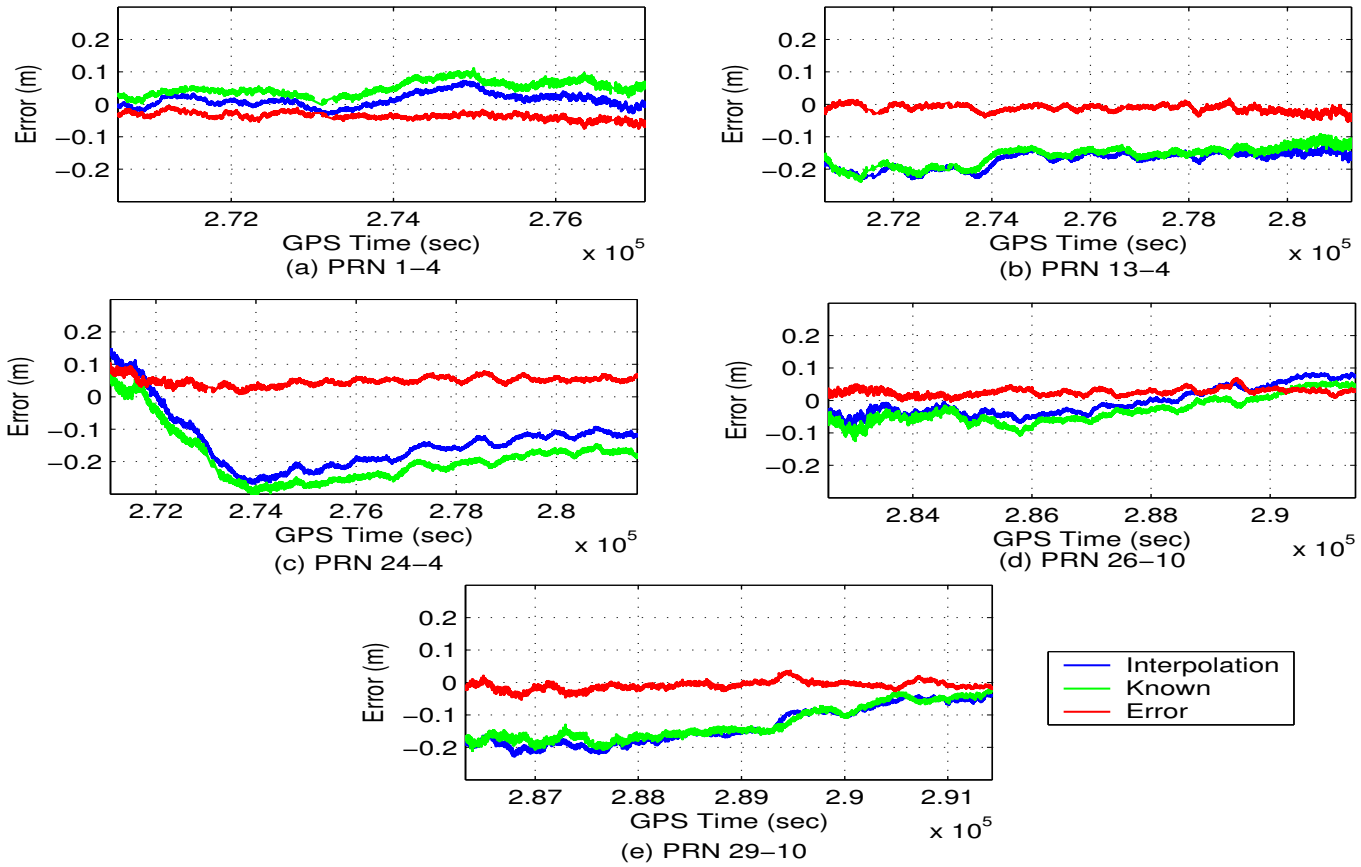

PRN	1 - 4	13 - 4	24 - 4	26 - 10	29 - 10
MAX (m)	-0.075	-0.054	0.103	0.069	-0.054
STDEV (m)	0.011	0.011	0.013	0.011	0.013
MEAN (m)	-0.036	-0.012	0.049	0.026	-0.001

2.5 Conclusion

- An approach using altitude-aiding and using a wide-lane search before stepping to L1 ambiguity search technique has been investigated
- A four-step strategy has been proposed to estimate the ionospheric delays using existent permanent and continuously operation GPS network.

3. Models and Parameters for GNSS

- Models
  - GNSS Positioning and Navigation Models
  - Stochastic Model
  - Solving the GNSS Model
  - Integrity Ambiguity Estimation
- Parameters
  - Ambiguity Success Rate
  - Internal Reliability and External Reliability
  - Parameters to Quantify Performance of GNSS

3.2 Positioning with the GNSS

- Generic Observation Equations

$$P^s_{r,i} = \rho^s_r + d_{r,i} - d^{s,i} + \mu_i I^s_r + T^s_r + M_{P^s_{r,i}} + \epsilon^s_{r,i}$$

$$\Phi^s_{r,i} = \rho^s_r + \delta_{r,i} - \delta^{s,i} - \mu_i I^s_r + T^s_r + \lambda_i N^s_{r,i} + M_{\Phi^s_{r,i}} + \varepsilon^s_{r,i}$$

  - Φ, P - carrier phase and pseudorange;
  - ρ - geometric range from satellite s to receiver r;
  - $i = L1$, $L2$, $L5$, $E1$, $E5a$, $E5b$, and $E6$;
  - $\mu_i = \frac{f^2_{L1}}{f^2_i}$, f is the frequency of the signal i;
  - I, T - ionospheric, tropospheric delay;
  - d, δ - satellite, receiver clock error;
  - M - multipath delay
  - λ, N - wavelength and ambiguity;
  - ϵ, ε - effect of receiver noise.

3.2 Carrier Phase Based Positioning

- Generic Equation of the Three Carrier Phase Based Positioning Models

$$y = \begin{bmatrix} \mathcal{I}_k \otimes \mathcal{M} & e_k \otimes \mathcal{N} \end{bmatrix} \begin{bmatrix} b \\ a \end{bmatrix} + n$$

  - y - the 'observed minus computed' double difference observations, accumulated over k epoches;
  - a - the component of ambiguities;
  - n - the noise vector;
  - $\mathcal{I}_k$ - an identity matrix of order k;
  - e_k - a vector consisting of k ones;
  - $\otimes$ - Kronecker product.
- Different Models: $\mathcal{M}$, $\mathcal{N}$ and b.

3.2 Carrier Phase Based Positioning

- Geometry-free (GF) Model
  $\mathcal{M} = e_\eta \otimes \mathcal{I}_{m-1}$, $\mathcal{N} = C_2 \otimes \mathcal{I}_{m-1}$, and $b \Rightarrow \rho$
- Roving-receiver Geometry-based (RR) Model
  $\mathcal{M} = e_\eta \otimes \bar{G}$, $\mathcal{N} = C_2 \otimes \mathcal{I}_{m-1}$, and
  $b \Rightarrow 3k$ baseline increments $\Delta \mathrm{b}_k$.
- Stationary-receiver Geometry-based (SR) Model
  $\mathcal{M} = \emptyset$, $\mathcal{N} = \left[e_\eta \otimes \bar{G} \;\; C_2 \otimes \mathcal{I}_{m-1}\right]$, and
  $b \Rightarrow$ 3 baseline increments $\Delta \mathrm{b}$.
  - $\eta = 2\zeta$ (code & phase), otherwise $\eta = \zeta$;
  - ζ - the number of observed signals;
  - m - the observing satellite number;
  - $C_2 = c_2 \otimes \mathcal{I}_\zeta$, and c_j denotes a vector with a one at the j-th entry and zeros otherwise.

3.3 Stochastic Model

- Single Difference Variance-covariance Matrix

$$C_{P\Phi} = \begin{bmatrix} C_P & \\ & C_\Phi \end{bmatrix}$$

- Double Difference Variance-covariance Matrix

$$Q_y = \mathcal{I}_k \otimes C_{P\Phi I} \otimes E$$

  - $C_{P\Phi I} = C_{P\Phi} + 2s^2 \begin{bmatrix} \mu \\ -\mu \end{bmatrix} \begin{bmatrix} \mu \\ -\mu \end{bmatrix}^T$
    - $\mu = \left(\mu_{i(1)}, \cdots, \mu_{i(\zeta)}\right)^T$, $\mu_i = \frac{f_{L1}^2}{f_i^2}$
    - s^2 - the undifferenced ionospheric weighting factor

$s^2 = 0$	$0 < s^2 < \infty$	$s^2 \to \infty$
Ionosphere-fixed	Ionosphere-weighted	Ionosphere-float

  - $E = D^T D$, D^T is the double difference operator.

3.4 Solving the GNSS Model

- Float Solution: $\min_{a,b} \|y - Aa - Bb\|^2_{Q_y^{-1}}$ with $a \in R^q$, $b \in R^p$
  - Float solution: $\begin{bmatrix} \hat{a} \\ \hat{b} \end{bmatrix}, \quad \begin{bmatrix} Q_{\hat{a}} & Q_{\hat{a}\hat{b}} \\ Q_{\hat{b}\hat{a}} & Q_{\hat{b}} \end{bmatrix}$
- Ambiguity Resolution: $\min_{a} \|\hat{a} - a\|^2_{Q_{\hat{a}}}$, with $a \in Z^q$
  - $\breve{a} = \mathbf{M}(\hat{a})$, with $\mathbf{M} : R^q \mapsto Z^q$
    - Integer Rounding
    - Integer Bootstrapping
    - Integer Least Squares
- Fixed Solution: $\min_{b} \left\| \hat{b}_{|a} - b \right\|^2_{Q_{\hat{b}|\hat{a}}}, \; b \in R^q$
  - $\breve{b} = \hat{b} - Q_{\hat{b}\hat{a}} Q_{\hat{a}}^{-1} (\hat{a} - \breve{a})$

3.5.1 Integer Rounding

- Integer Rounding Estimator

$$\breve{a}_R = \begin{bmatrix} [\hat{a}_1]_{roundoff} \\ [\hat{a}_2]_{roundoff} \\ \vdots \\ [\hat{a}_n]_{roundoff} \end{bmatrix}$$

where $[\cdot]_{roundoff}$ denotes rounding a real number to its nearest integer

- Integer rounding estimator does not take correlation between the elements of the integer ambiguity vector in account.
- This only is the case when the ambiguity variance covariance matrix $Q_{\hat{a}}$ is a diagonal matrix.

3.5.2 Integer Bootstrapping

- Integer Bootstrapping Estimator

$$\breve{a}_B = \begin{bmatrix} [\hat{a}_1]_{roundoff} \\ \left[\hat{a}_2 - \sigma_{\hat{a}_2\hat{a}_1}\sigma_{\hat{a}_1}^{-2}\left(\hat{a}_1 - \breve{a}_{B,1}\right)\right]_{roundoff} \\ \vdots \\ \left[\hat{a}_n - \sum_{i=1}^{n-1}\sigma_{\hat{a}_n\hat{a}_{i|I}}\sigma_{\hat{a}_{i|I}}^{-2}\left(\hat{a}_{i|I} - \breve{a}_{B,i}\right)\right]_{roundoff} \end{bmatrix}$$

- Integer Bootstrapping Estimator takes some of the ambiguity correlation into account.
- The bootstrapped estimator is not unique. The integer solution depends on with which ambiguity the bootstrapping is started.

3.5.3 Integer Least Squares

- Integer Least Squares Estimator

$$\breve{a}_{LSQ} = \arg \min_{a \in Z^q} (\hat{a} - a)^T Q_{\hat{a}}^{-1} (\hat{a} - a)$$

- It is a nonstandard least-squares problem due to the integer constraints $a \in Z^q$.
- LAMBDA method

1) Transform the ambiguity vector and vc-matrix with decorrelation matrix Z^T

$$\hat{z} = Z^T \hat{a}, \; Q_{\hat{z}} = Z^T Q_{\hat{a}} Z$$

2) Search the transformed integer ambiguities in the transformed ambiguities domain

$$\Omega_z = \left\{ z \in Z^q | \, (\hat{z} - z)^T Q_{\hat{z}}^{-1} (\hat{z} - z) \leq \chi^2 \right\}$$

3) Original ambiguities: $\breve{a} = Z^{-T} \breve{z}$

3. Models and Parameters for GNSS

- Models
  - GNSS Positioning and Navigation Models
  - Stochastic Model
  - Solving the GNSS Model
  - Integrity Ambiguity Estimation
- ***Parameters***
  - Ambiguity Success Rate (ASR)
  - Internal Reliability
    - Minimal Detectable Bias (MDB)
  - External Reliability
    - Bias-to-Noise Ratio (BNR)
    - Minimal Detectable Effect (MDE)
  - Parameters to Quantify Performance of GNSS

3.6 Ambiguity Success Rate

- Ambiguity Success Rate: the probability that the integer ambiguities are correctly estimated
  - $P(\breve{a} = a) = \int_{S_a} p_{\hat{a}}(x)dx$
    - $p_{\hat{a}}(x)$: the probability density function of the float ambiguities;
    - S_a is the pull-in region.
- Three Contributing Factors

(1) Function model: GF, RR or SR model

(2) Stochastic model: Q_y

(3) Integer ambiguity estimator: $\breve{a}_R$, $\breve{a}_B$ and $\breve{a}_{LS}$

3.6.3 ASR Closed-form Expression

- It is very difficult to evaluated the integer normal distribution, because of the complicated geometry of the pull-in region.
  - A Diagonal Ambiguity Variance-covariance Matrix

$$\mathbf{P}\left(\check{a}_{Q_{\hat{a}}=diag}=a\right)=\prod_{i=1}^{q}\left[2\Phi\left(\frac{1}{2\sigma_{\hat{a}_i}}\right)-1\right]$$

  - Integer Bootstrapping

$$\mathbf{P}\left(\check{a}_{B}=a\right)=\prod_{i=1}^{q}\left[2\Phi\left(\frac{1}{2\sigma_{\hat{a}_{i|I}}}\right)-1\right]$$

- Bounding the ASR

$$\mathbf{P}\left(\check{a}_{R}=a\right)\leq\mathbf{P}\left(\check{a}_{B}=a\right)\leq\mathbf{P}\left(\check{a}_{LSQ}=a\right)$$

3.7.1 Internal Reliability

- Internal Reliability describes the size of the model errors which can just be detected with the appropriate test statistics.
- The uniformly most powerful test statistic for testing H_0 against H_a is given as

$$\mathbf{T} = \frac{\left(c^T Q_y^{-1} \mathcal{P}_{\mathcal{A}}^{\perp} y\right)^2}{c^T Q_y^{-1} \mathcal{P}_{\mathcal{A}}^{\perp} c}$$

  - $H_0 : E\{y\} = \mathcal{A}x, \qquad D\{y\} = Q_y$
  - $H_a : E\{y\} = \mathcal{A}x + c\nabla, \quad D\{y\} = Q_y$

- The test statistic $\mathbf{T}$ has the following Chi-squared distributions under H_0 and H_a

$H_0 : \ T \sim \chi^2(1,0); \quad H_a : \ T \sim \chi^2(1,\lambda)$

where $\lambda = \nabla^2 c^T Q_y^{-1} \mathcal{P}_{\mathcal{A}}^{\perp} c$

3.7.1 Internal Reliability

- $\lambda = \nabla^2 c^T Q_y^{-1} \mathcal{P}_{\mathcal{A}}^{\perp} c$

  A level of significance of α_0 together with a detection power of γ_0 will give a non-centrality parameter of $\lambda_0 = \lambda(\alpha_0,\ \gamma_0)$

- Minimal Detectable Bias (MDB)

  $$|\nabla| = \sqrt{\frac{\lambda_0}{c^T Q_y^{-1} \mathcal{P}_{\mathcal{A}}^{\perp} c}}$$

  - A Code Outlier

    $$\left|\nabla_{P_{r,i}^s}\right| = \sqrt{\frac{\lambda_0}{d^T Q_y^{-1}\left(\mathcal{I}_{m-1} - \left(1-\frac{1}{k}\right)\mathcal{P}_{\mathcal{M}} - \frac{1}{k}\left(\mathcal{P}_{\mathcal{N}} + \mathcal{P}_{P_{\mathcal{N}}^{\perp}\mathcal{M}}\right)\right) d}}$$

  - A Cycle Slip

    $$\left|\nabla_{\Phi_{r,i}^s}\right| = \sqrt{\frac{\lambda_0}{v \cdot d^T Q_y^{-1}\left(\mathcal{I}_{m-1} - \left(1-\frac{v}{k}\right)\mathcal{P}_{\mathcal{M}} - \frac{v}{k}\mathcal{P}_{\mathcal{N}}\right) d}}$$

3.7.2 External Reliability

- External Reliability: the influence of a bias with the size of the MDB on the estimated parameters, $\hat{x}$,
  $\nabla\hat{x} = \left(\mathcal{A}^T Q_y^{-1}\mathcal{A}\right)\mathcal{A}^T Q_y^{-1} c\nabla = Q_{\hat{x}}\mathcal{A}^T Q_y^{-1} c\nabla$
  - Bias-to-Noise Ratio (BNR): $\sqrt{\lambda_{\hat{x}}}$
    $\lambda_{\hat{x}} = \|\nabla\hat{x}\|^2_{Q^{-1}_{\hat{x}}} = \|\mathcal{P}_{\mathcal{A}} c\nabla\|^2_{Q^{-1}_{\hat{x}}}$
  - Minimal Detectable Effect (MDE)
    $$MDE = \sqrt{\left(\nabla\hat{b}_1\right)^2 + \left(\nabla\hat{b}_2\right)^2 + \left(\nabla\hat{b}_3\right)^2}$$
    where $\nabla\hat{b}_i$ are the entries of $\nabla\hat{b}$ that refer to the position unknowns.

3.8 GNSS Performance Parameters

- Availability: Number of Visible Satellites (NVS)
- Accuracy: GDOP
- Reliability
  - Internal Reliability: MDB
  - External Reliability: BNR/MDE
- Capability of Carrier Phase Based Positioning and Navigation: Ambiguity Success Rate (ASR)

$$\left.\begin{array}{r} \textbf{NVS} \uparrow \\ \textbf{GDOP} \downarrow \\ \textbf{MDB} \downarrow \\ \textbf{BNR/MDE} \downarrow \\ \textbf{ASR} \uparrow \end{array}\right\} \Rightarrow \textbf{Performance} \uparrow$$

4. Hybrid GPS and Galileo Positioning

- GPS Modernization and Galileo System
  - Satellite Constellation
  - Signal Structure
- Performance Analysis
  - Configuration
  - Spatial Variation
  - Temporal Variation

4.2/4.3 Satellite Constellations

System	Number of Satellites	Orbital Planes	Inclination	Semi-major Axis
GPS	24	6 MEO	55°	26,560 km
Galileo	27/3	3 MEO	56°	29,994 km

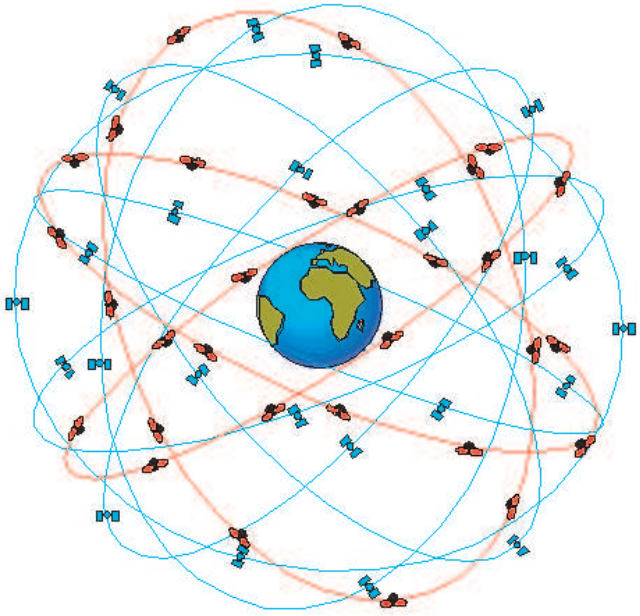

Parameters of Galileo satellite constellation (*Walker* constellation)

Semi-major Axis (a)	29,994 km
Inclination (i)	56°
Right Ascension ($\Omega_\circ$)	-120°, 0°, 120°
Rate of Right Ascension ($\dot{\Omega}$)	0.0°/day
Argument of Perigee(ω)	0.0°
Mean Anomaly ($M_\circ$) (1^{st} orbit plan)	-160°, -120°, $\cdots$, 120°, 160°

4.2/4.3 Signal Structures

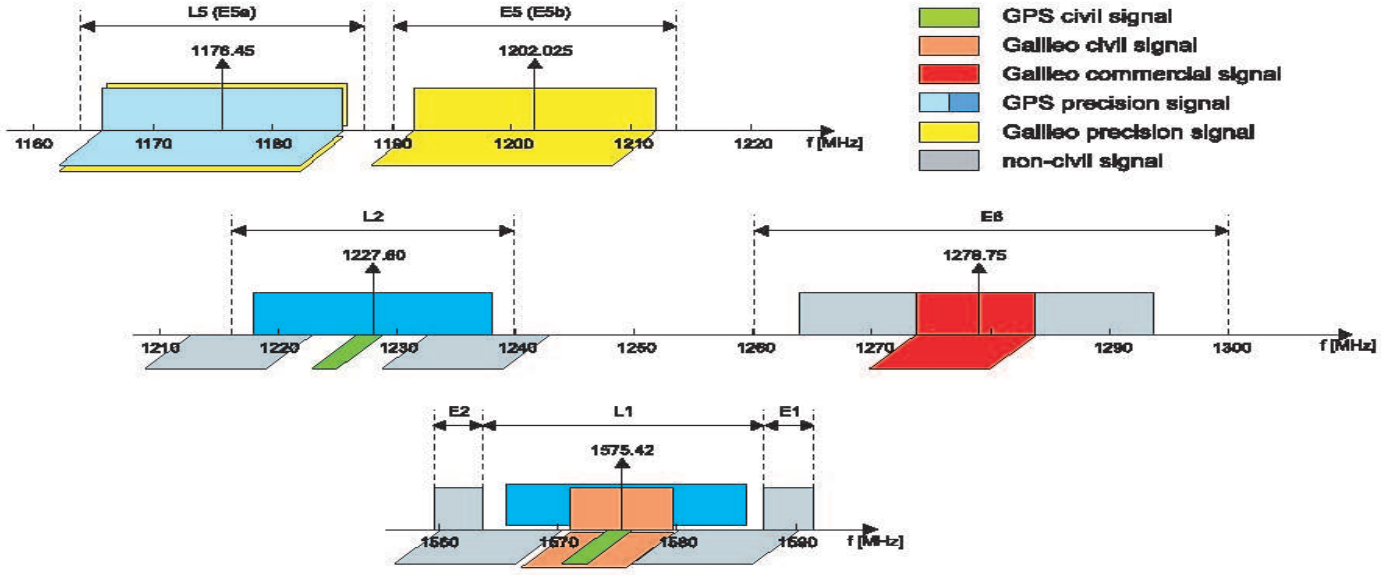

Signal	f(10.23MHz)	λ(cm)	C/N$_0$(dBHz)	Modulation	Data rate	σ_P(m)
L1	154	19.03	47.3	BPSK(1)	50bps	0.300
L2	120	24.42	45	BPSK(1)	50bps	0.300
L5	115	25.48	51	BPSK(10)	I:100sps, Q:DF	0.100
E1	154	19.03	50	BOC(2,2)	B:200sps, C:DF	0.300
E5a	115	25.48	50	BPSK(10)	I:50sps, Q:DF	0.300
E5b	117.5	24.94	50	BPSK(10)	I:50sps, Q:DF	0.200
E6	125	23.44	47	BPSK(5)	DF	0.200

4.4 Performance Analysis

System		GPS, Galileo, and GPS+Galileo
Functional Model	Baseline Model	Single medium length baseline (20 km), RR model
	Elevation Mask	15° or 30°
	Number of Epoches	Signal epoch
	Number of Signals	dual-/triple-frequency
Stochastic Model	Code	$\sigma_P = 0.300$ m
	Phase	$\sigma_\Phi = 0.003$ m
	Ionospheric Model	Ionosphere-weighted model, $\sigma_I = 0.020$ m
	Tropospheric Delay	$\sigma_T = 0.010$ m
Integer Ambiguity Estimation		Bootstrapped estimator
Spatial Simulation	Date and Time	February 9, 2004, 12:00
	Location	Asia-Pacific and Australian area (Grid: $0.4^\circ \times 0.4^\circ$)
Temporal Simulation	Date and Time	2004-02-08, 00:00 - 2004-02-14, 24:00 (120 sec)
	Location	Sapporo/Tokyo/Fukuoka/Beijing/Shanghai/Hongkong
Output	Spatial Variation	NVS, GDOP, ASR, MDB (for L1 or E1 code outlier), BNR and MDE
	Temporal Variation	

4.4.1 Spatial Variations of NVS

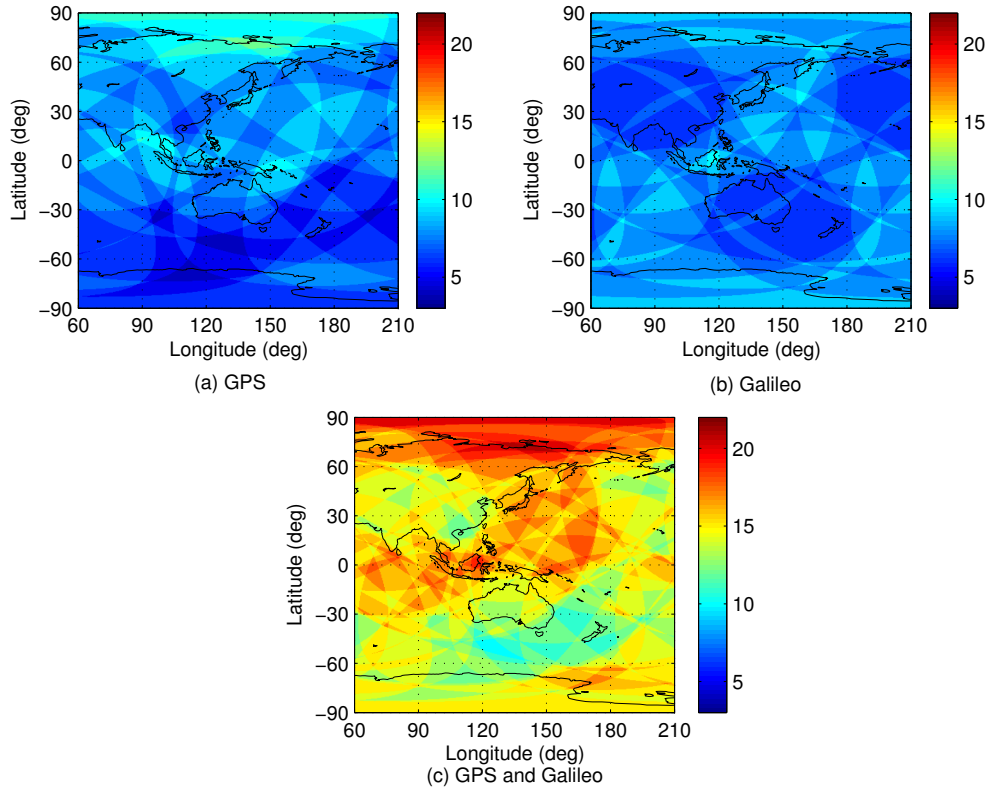

System ($15°$)		GPS	Galileo	GPS + Galileo
Whole Area	NVS ≥ 4	100.00%	100.00%	100.00%
Positioning Available Area ($\mathrm{NVS}_{\mathtt{All}} \geq 4$)	MIN	4	5	10
	MEAN	7.51	7.58	15.09
	MAX	12	10	21

4.4.1 Spatial Variations of GDOP

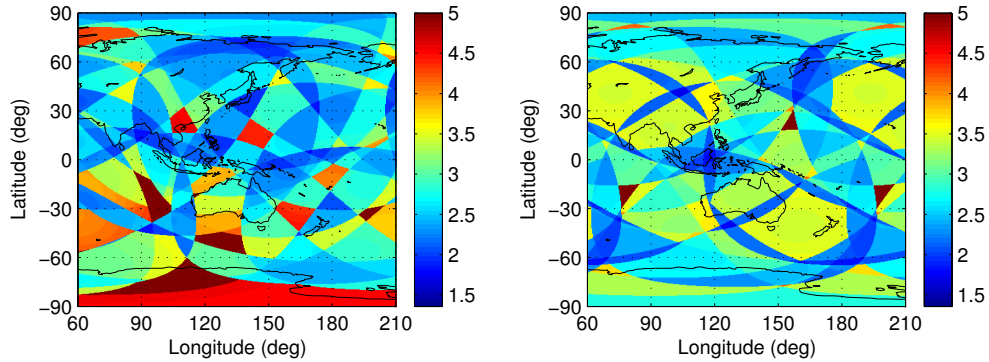

(a) GPS

(b) Galileo

(c) GPS and Galileo

System ($15°$)		GPS	Galileo	GPS + Galileo
Whole area	NVS ≥ 4	100.00%	100.00%	100.00%
Positioning available area ($\text{NVS}_{\texttt{All}} \geq 4$)	MIN	1.69	1.74	1.36
	MEAN	3.19	2.86	1.90
	MAX	27.80	8.26	3.50

4.4.1 Spatial Variations of ASR (Dual)

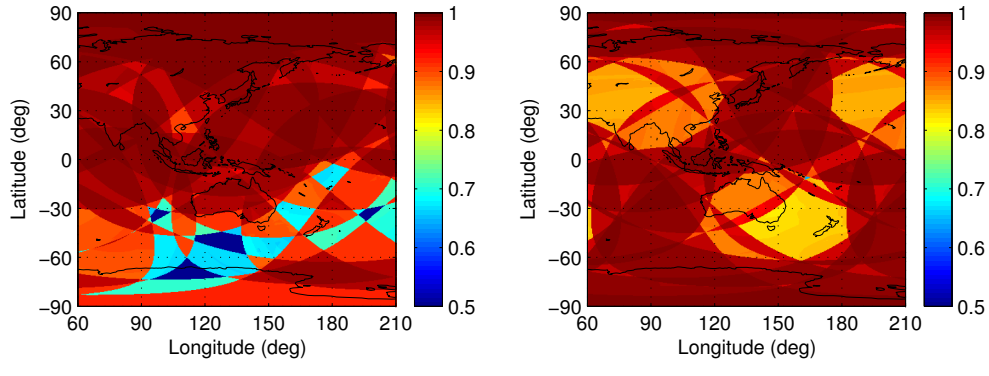

(a) GPS

(b) Galileo

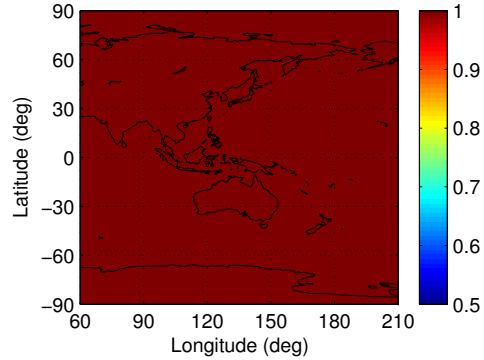

(c) GPS and Galileo

System ($15°$)		GPS	Galileo	GPS + Galileo
Whole Area	NVS ≥ 4	100.00%	100.00%	100.00%
Positioning	MIN	28.93%	64.54%	99.24%
Available Area	MEAN	92.95%	95.57%	99.82%
($\mathrm{NVS}_{\mathtt{All}} \geq 4$)	MAX	99.81%	99.83%	99.90%

4.4.1 Spatial Variations of ASR (Triple)

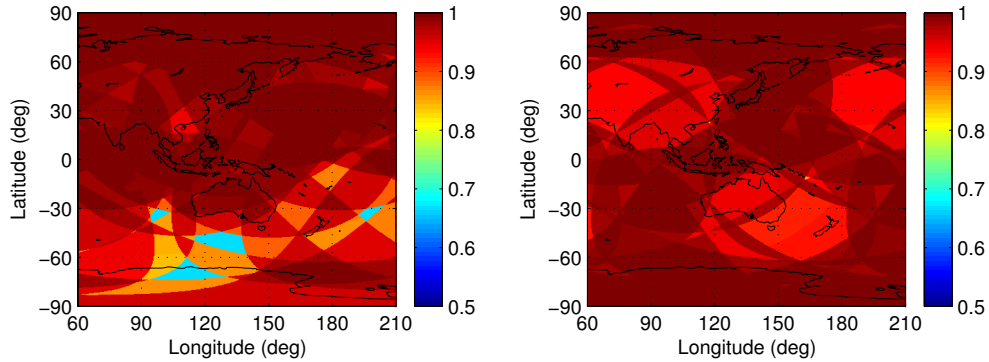

(a) GPS

(b) Galileo

(c) GPS and Galileo

System ($15°$)		GPS	Galileo	GPS + Galileo
Whole Area	NVS ≥ 4	100.00%	100.00%	100.00%
Positioning Available Area ($\text{NVS}_{\text{All}} \geq 4$)	MIN	66.97%	84.02%	99.42%
	MEAN	96.74%	97.89%	99.87%
	MAX	99.92%	99.86%	99.93%

4.4.1 Spatial Variations of MDB

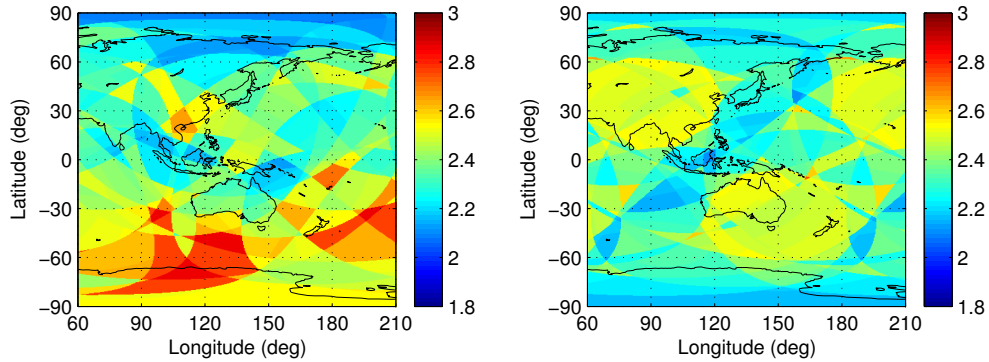

(a) GPS

(b) Galileo

(c) GPS and Galileo

System ($15°$)		GPS	Galileo	GPS + Galileo
Whole Area	NVS ≥ 4	100.00%	100.00%	100.00%
Positioning available area ($\text{NVS}_{\texttt{All}} \geq 4$)	MIN	2.08	2.11	1.95
	MEAN	2.42	2.35	2.12
	MAX	2.86	2.77	2.43

4.4.1 Spatial Variations of BNR

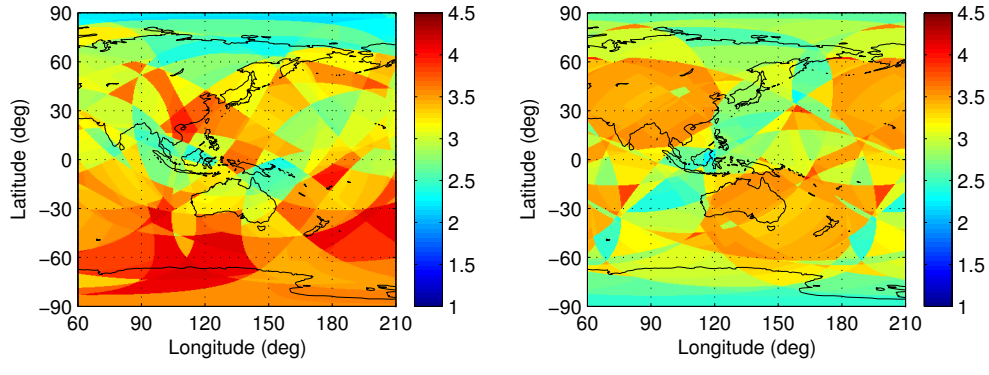

(a) GPS

(b) Galileo

(c) GPS and Galileo

System ($15°$)		GPS	Galileo	GPS + Galileo
Whole Area	NVS ≥ 4	100.00%	100.00%	100.00%
Positioning Available Area ($\mathrm{NVS}_{\mathtt{All}} \geq 4$)	MIN	2.17	2.25	1.25
	MEAN	3.25	3.07	2.06
	MAX	4.13	4.12	3.03

4.4.1 Summary of Spatial Variations

System ($15°$)			GPS	Galileo	GPS + Galileo
Whole Area	NVS ≥ 4		100.00%	100.00%	100.00%
Positioning Available Area ($NVS_{All} \geq 4$)	NVS	MAX	12	10	21
		MEAN	7.51	7.58	15.09
	GDOP	MIN	1.69	1.74	1.36
		MEAN	3.19	2.86	1.90
	ASR (Dual)	MAX	99.81%	99.83%	99.90%
		MEAN	92.95%	95.57%	99.82%
	ASR (Triple)	MAX	99.92%	99.86%	99.93%
		MEAN	96.74%	97.89%	99.87%
	MDB	MIN	2.08	2.11	1.95
		MEAN	2.42	2.35	2.12
	BNR	MIN	2.17	2.25	1.25
		MEAN	3.25	3.07	2.06
	MDE	MIN	0.16	0.21	0.08
		MEAN	1.09	0.86	0.38

4.4.2 Temporal Variations of NVS

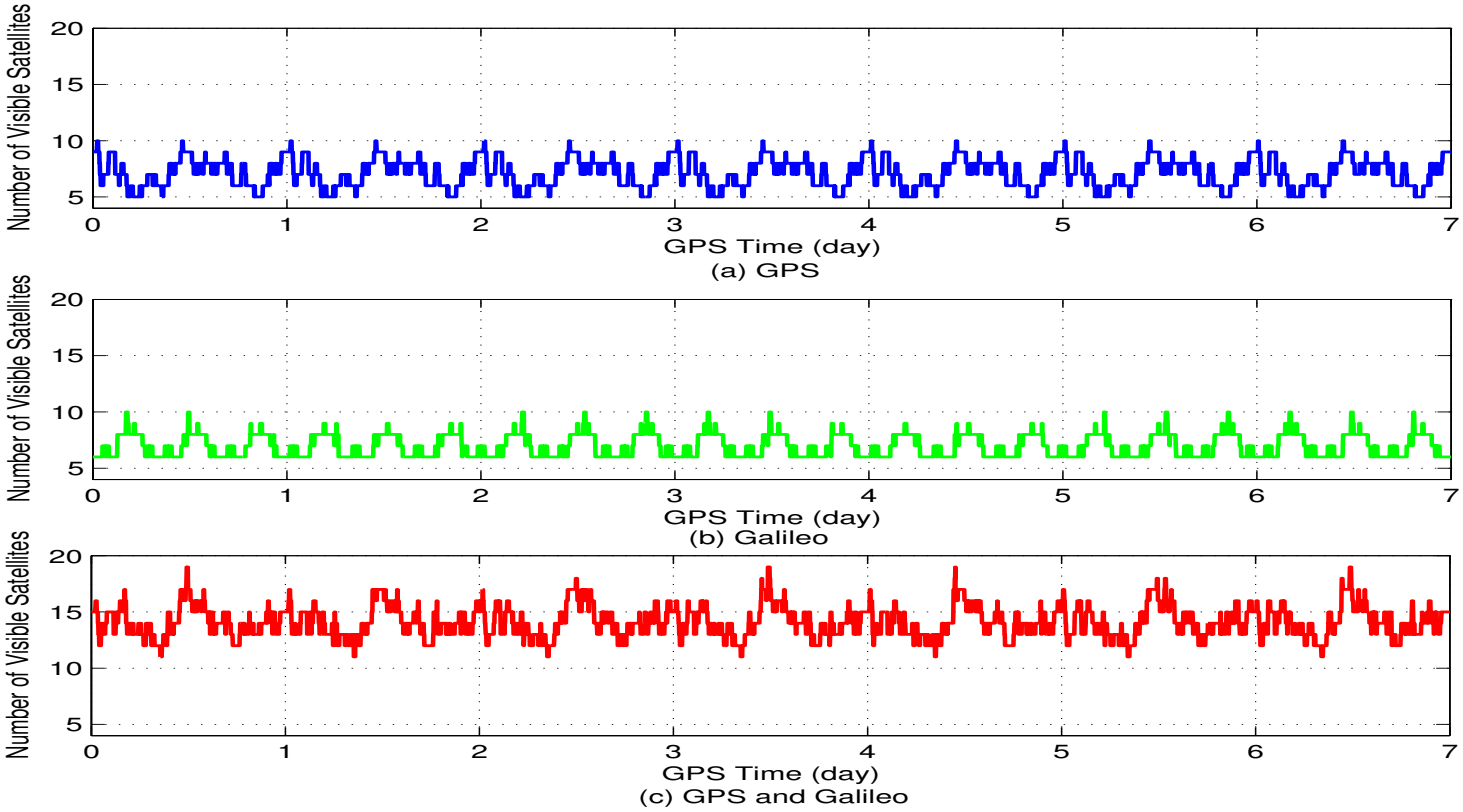

System (Tokyo, $15°$)		GPS	Galileo	GPS + Galileo
Whole Time	NVS ≥ 4	100.00%	100.00%	100.00%
Positioning Available Time ($NVS_{All} \geq 4$)	MIN	5	6	11
	MEAN	7.12	6.99	14.11
	MAX	10	10	19

4.4.2 Temporal Variations of GDOP

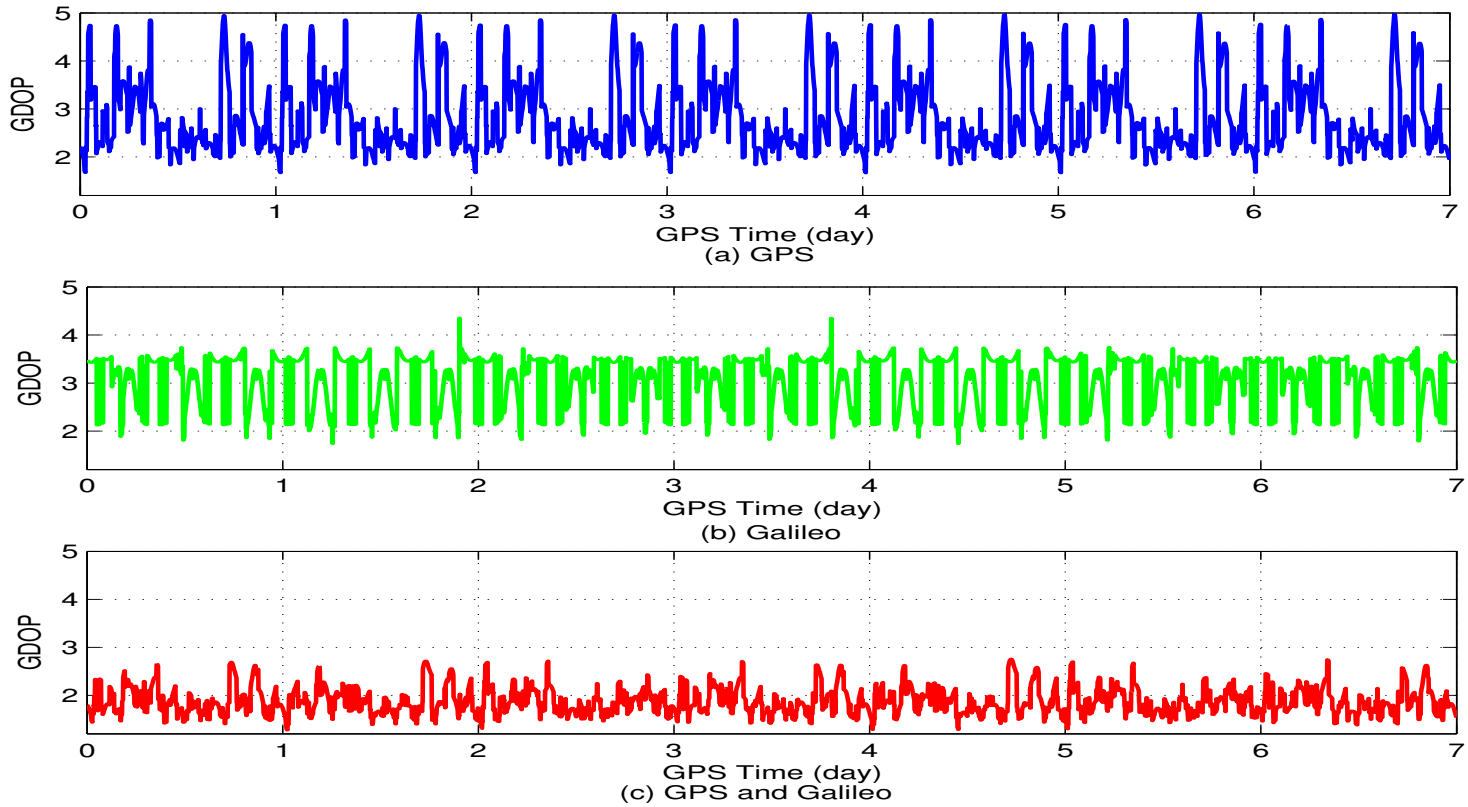

System (Tokyo, $15°$)		GPS	Galileo	GPS + Galileo
Whole Time	NVS ≥ 4	100.00%	100.00%	100.00%
Positioning Available Time ($NVS_{All} \geq 4$)	MIN	1.67	1.74	1.28
	MEAN	2.82	3.05	1.88
	MAX	4.98	4.35	2.75

4.4.2 Temporal Variations of ASR (Dual)

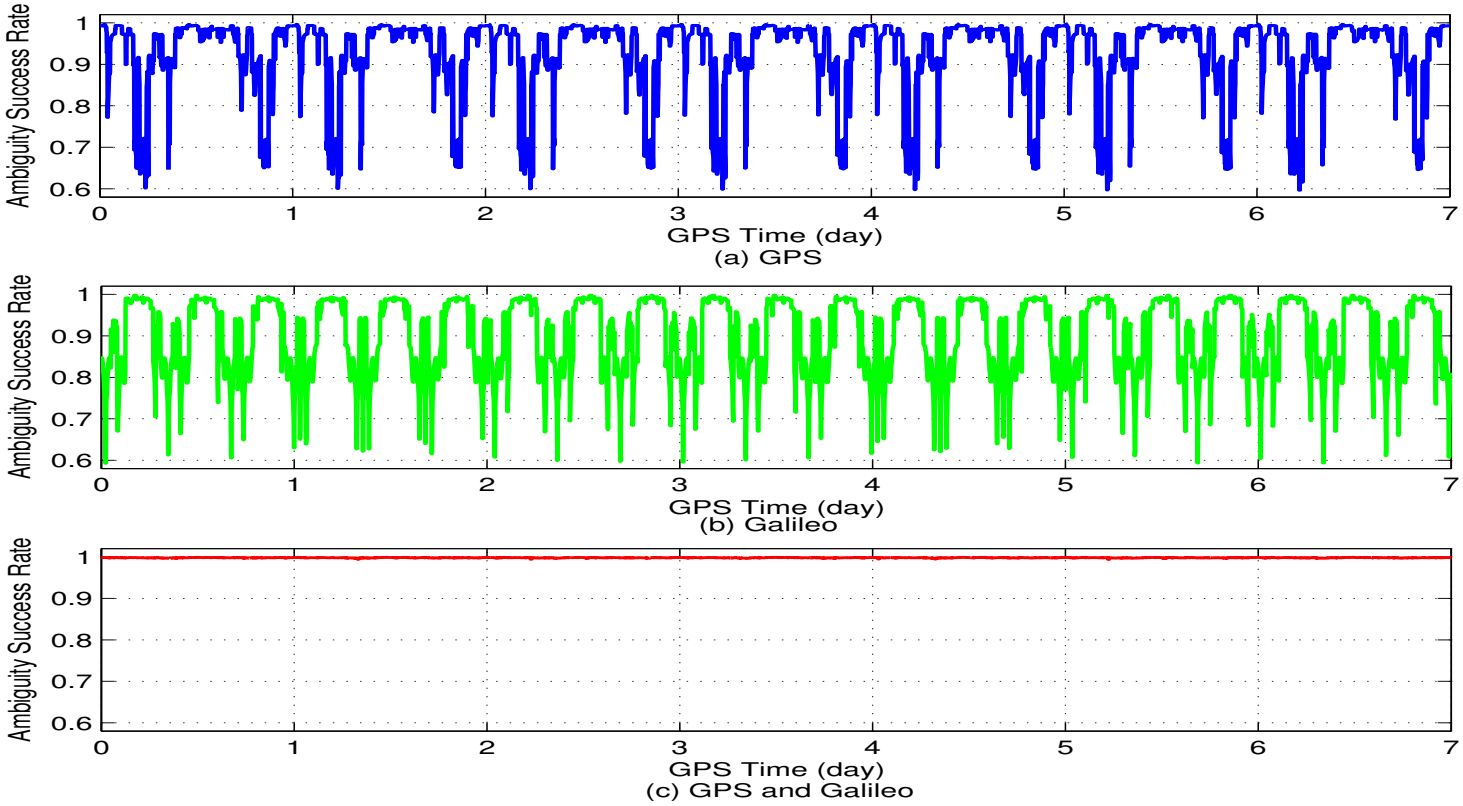

System (Tokyo, $15°$)		GPS	Galileo	GPS + Galileo
Whole Time	NVS ≥ 4	100.00%	100.00%	100.00%
Positioning	MIN	59.63%	59.23%	99.35%
Available Time	MEAN	92.67%	89.90%	99.80%
($\mathrm{NVS}_{\mathtt{All}} \geq 4$)	MAX	99.67%	99.82%	99.90%

4.4.2 Temporal Variations of ASR(Triple)

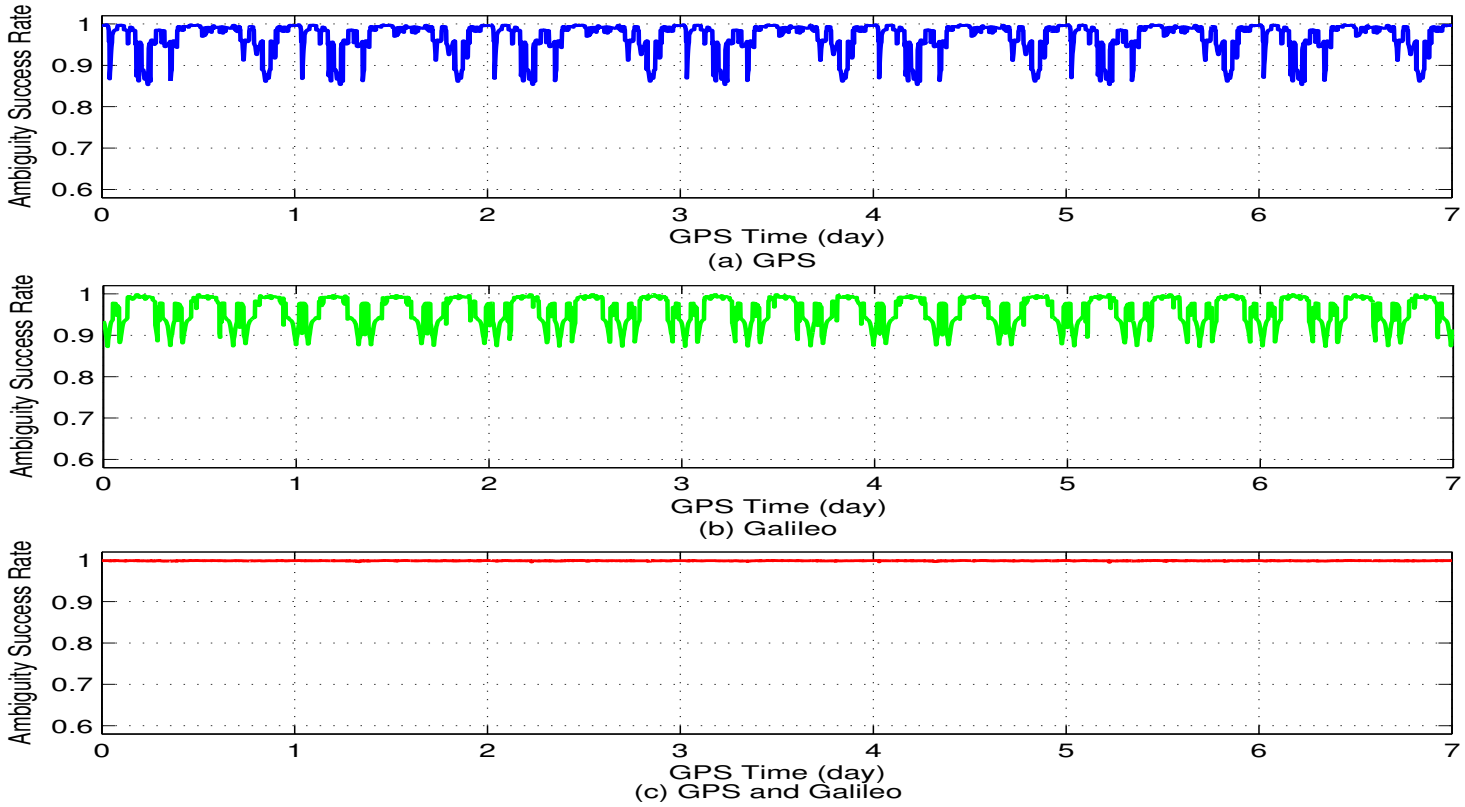

System (Tokyo, $15°$)		GPS	Galileo	GPS + Galileo
Whole Time	NVS ≥ 4	100.00%	100.00%	100.00%
Positioning	MIN	85.31%	87.24%	99.49%
Available Time	MEAN	96.71%	95.85%	99.86%
($NVS_{All} \geq 4$)	MAX	99.86%	99.86%	99.93%

4.4.2 Temporal Variations of MDB

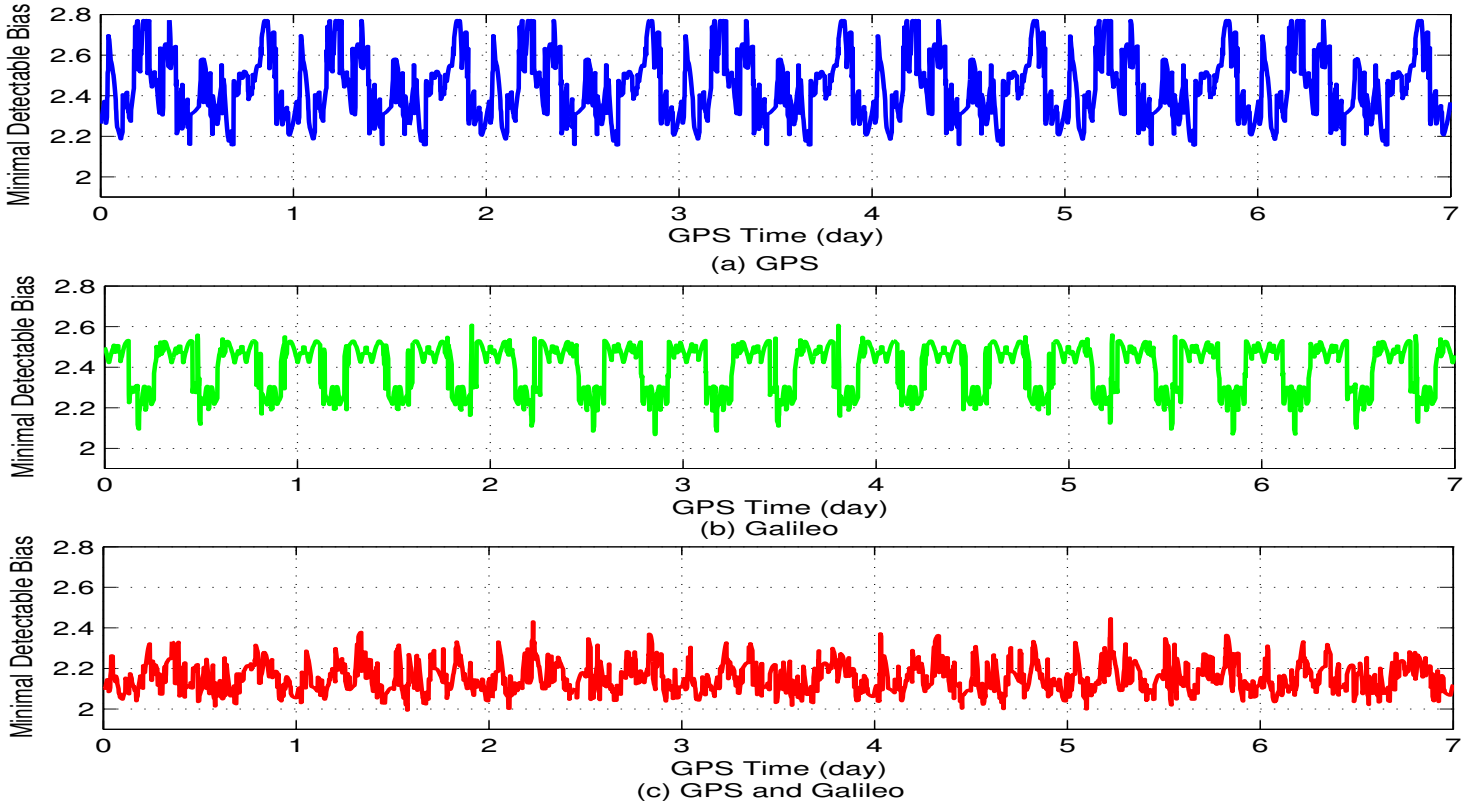

System (Tokyo, $15°$)		GPS	Galileo	GPS + Galileo
Whole Time	NVS ≥ 4	100.00%	100.00%	100.00%
Positioning Available Time ($NVS_{All} \geq 4$)	MIN	2.16	2.07	1.99
	MEAN	2.44	2.40	2.15
	MAX	2.77	2.61	2.45

4.4.2 Temporal Variations of BNR

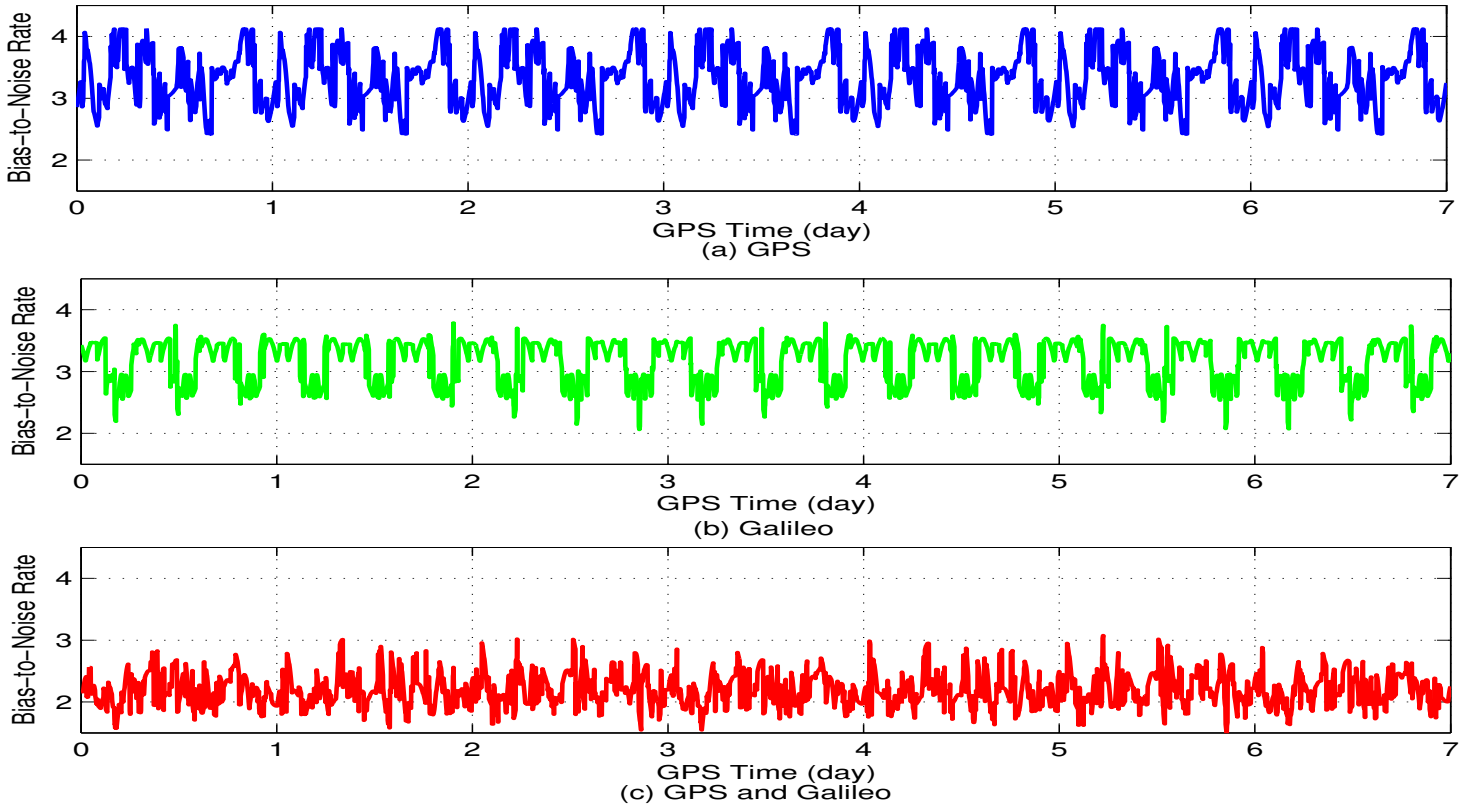

System (Tokyo, $15°$)		GPS	Galileo	GPS + Galileo
Whole Time	NVS ≥ 4	100.00%	100.00%	100.00%
Positioning	MIN	2.42	2.06	1.48
Available Time	MEAN	3.32	3.16	2.19
($\text{NVS}_{\texttt{All}} \geq 4$)	MAX	4.13	3.79	3.08

4.4.2 Summary of Temporal Variations

System (Tokyo, $15°$)			GPS	Galileo	GPS + Galileo
Whole Time	NVS ≥ 4		100.00%	100.00%	100.00%
Positioning Available Time ($NVS_{All} \geq 4$)	NVS	MAX	10	10	19
		MEAN	7.12	6.99	14.11
	GDOP	MIN	1.67	1.74	1.28
		MEAN	2.82	3.05	1.88
	ASR (Dual)	MAX	99.67%	99.82%	99.90%
		MEAN	92.67%	89.90%	99.80%
	ASR (Triple)	MAX	99.86%	99.86%	99.93%
		MEAN	96.71%	95.85%	99.86%
	MDB	MIN	2.16	2.07	1.99
		MEAN	2.44	2.40	2.15
	BNR	MIN	2.42	2.06	1.48
		MEAN	3.32	3.16	2.19
	MDE	MIN	0.27	0.27	0.14
		MEAN	1.10	1.00	0.45

4.5 Summary

- The performance of hybrid modernized GPS and Galileo has been investigated by software simulation;
- Performance Improvement
  - Availability;
  - Accuracy;
  - Capability of carrier phase based positioning and navigation;
  - Internal reliability and external reliability.

5. GPS Augmentation Using QZSS

- Japanese QZSS
  - Satellite Constellation
  - Signal Structure
- Performance Analysis
  - Performance Parameter
  - Spatial Variations
  - Temporal Variations

5.2.1 QZSS Satellite Constellation

QZSS Option	1	2	3
Satellite number	3	3	3
Semi-major axis	42,164 km	42,164 km	42,164 km
Eccentricity	0.099	0.360	0.000
Inclination	$45.0°$	$52.6°$	$45.0°$
Ground track	Asymmetrical 8-shape	Egg-shape	Symmetrical 8-shape

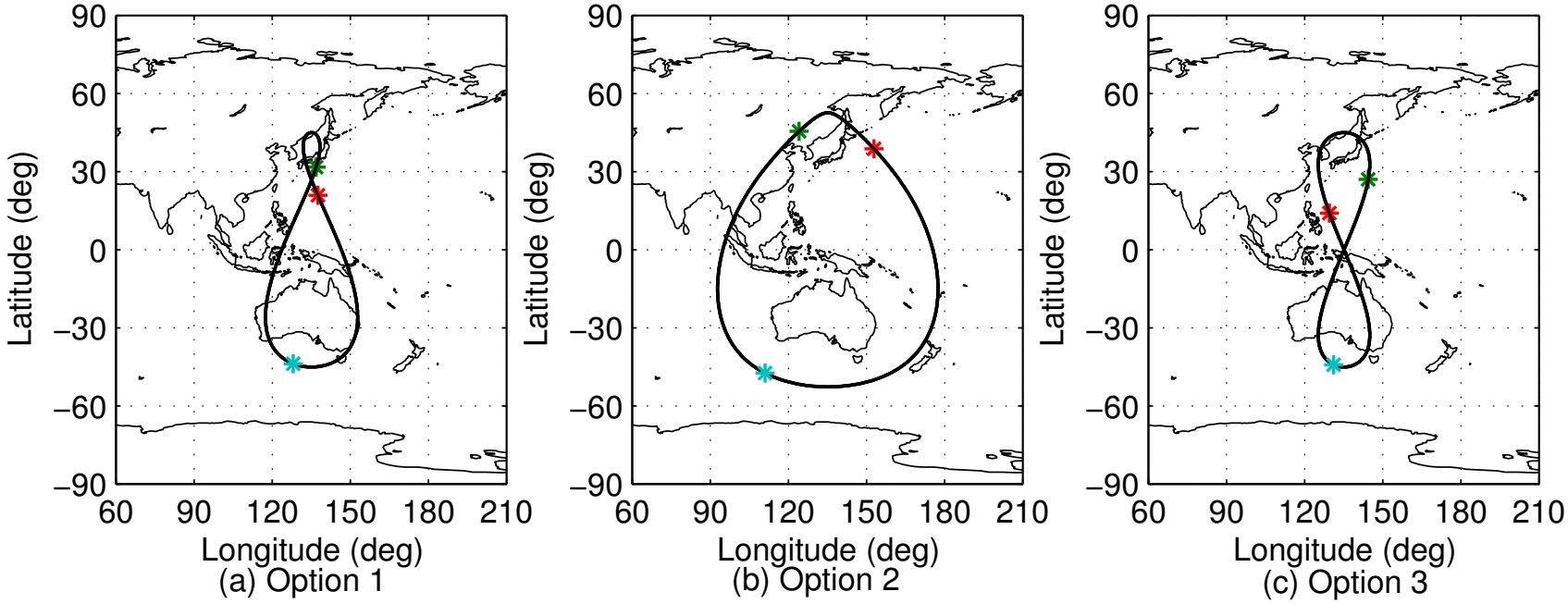

5.2.1 Temporal Elevation Variations

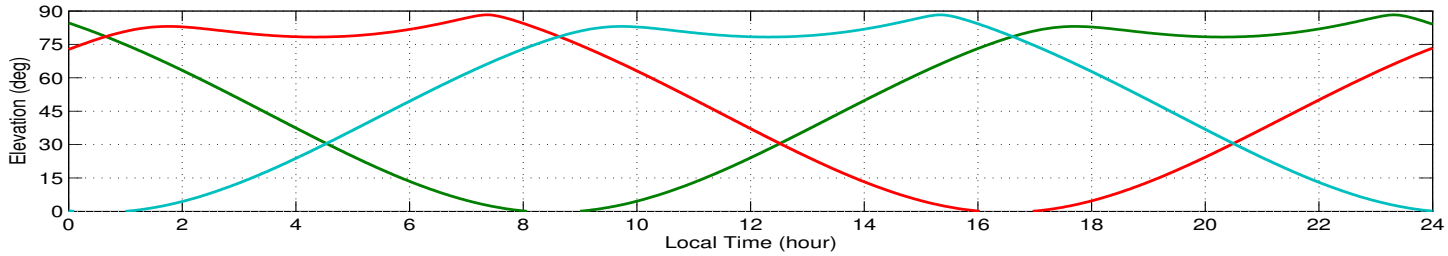

(a) QZSS Option 1

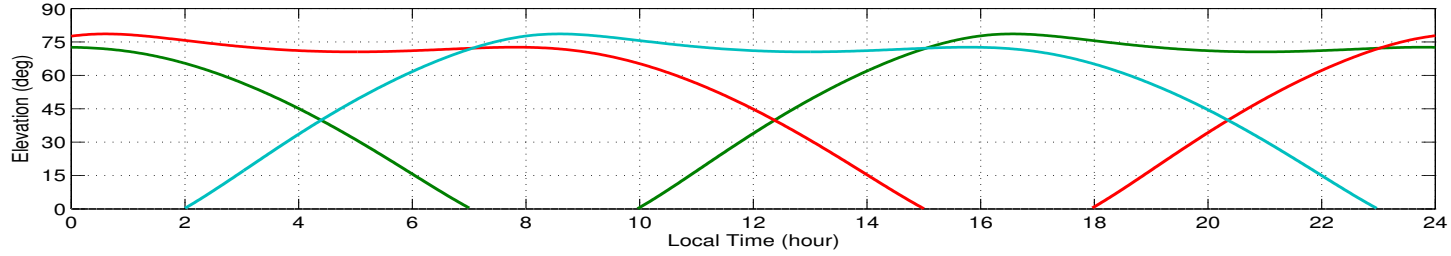

(b) QZSS Option 2

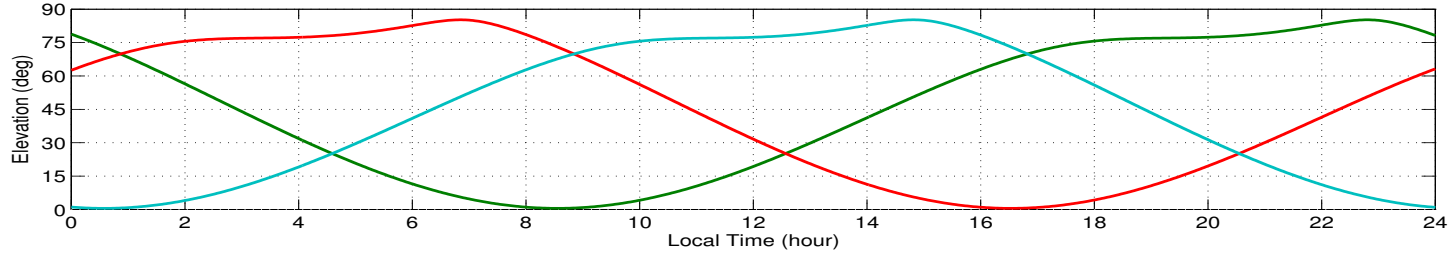

(c) QZSS Option 3

Location	Elevation Mask Angle	Number of Visible Satellites
Tokyo	30°	2
	70°	1

5.2.2 Signal Structure

- QZSS will use the same signal structure as GPS and employ pseudorandom noise code used by the GPS constellation and WAAS.

Signal	Frequency [MHz]	Wavelength [m]	σ_{code} [m]
L1	1575.42	0.1903	0.30
L2	1227.60	0.2442	0.30
L5	1176.45	0.2548	0.10

- Other types of signal modulations are also under consideration for the QZSS.

5.3 Performance Analysis

System		GPS, GPS+QZSS (Three options)
Functional Model	Baseline Model	Single medium length baseline (20 km), RR model
	Elevation Mask	15° or 30°
	Number of Epoches	Signal epoch
	Number of Signals	Dual-frequency
Stochastic Model	Code	$\sigma_P = 0.300$ m
	Phase	$\sigma_\Phi = 0.003$ m
	Ionospheric Model	Ionosphere-weighted model, $\sigma_I = 0.020$ m
	Tropospheric Delay	$\sigma_T = 0.010$ m
Integer Ambiguity Estimation		Bootstrapped estimator
Spatial Simulation	Date and Time	February 9, 2004, 12:00
	Location	Asia-Pacific and Australian area (Grid: $0.4^\circ \times 0.4^\circ$)
Temporal Simulation	Date and Time	2004-02-08, 00:00 - 2004-02-14, 24:00 (120 sec)
	Location	Sapporo/Tokyo/Fukuoka
Output	Spatial Variation	NVS, GDOP, ASR, MDB (for L1 code outlier), BNR and MDE
	Temporal Variation	

5.3.1 Spatial Variations of NVS

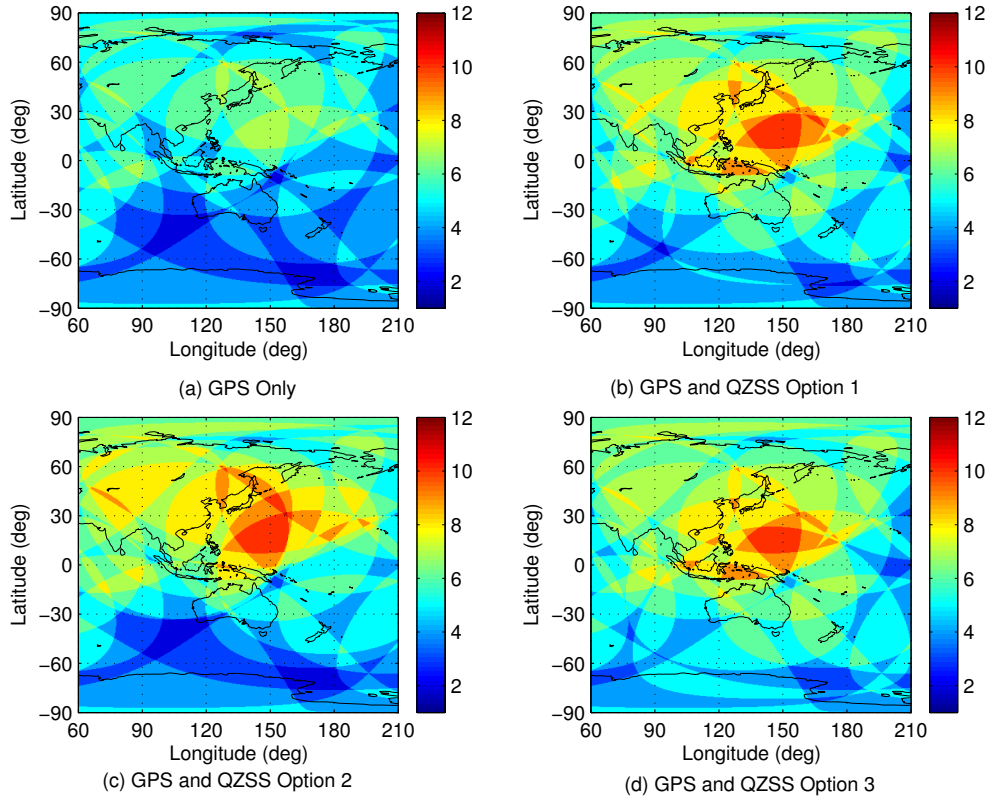

(a) GPS Only

(b) GPS and QZSS Option 1

(c) GPS and QZSS Option 2

(d) GPS and QZSS Option 3

System ($30°$)		GPS only	GPS+QZSS1	GPS+QZSS2	GPS+QZSS3
Whole Area	NVS ≥ 4	84.23%	95.85%	88.57%	96.96%
Positioning Available Area ($NVS_{All} \geq 4$)	MIN	4	4	4	4
	MEAN	5.00	6.16	6.20	6.15
	MAX	8	10	11	10

5.3.1 Spatial Variations of GDOP

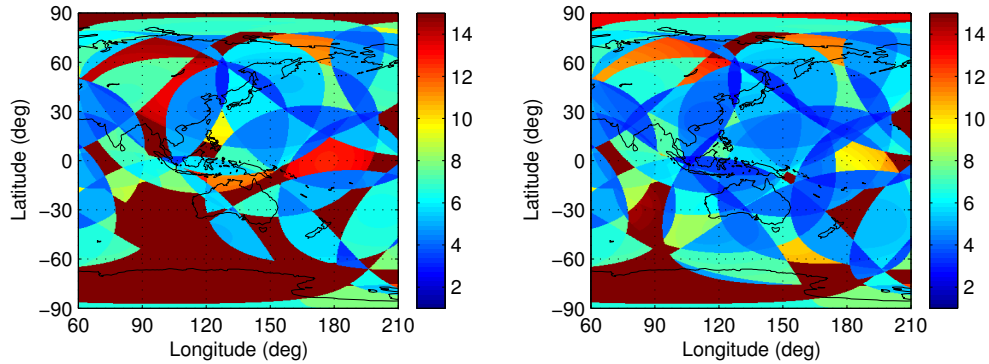

(a) GPS Only

(b) GPS and QZSS Option 1

(c) GPS and QZSS Option 2

(d) GPS and QZSS Option 3

System ($30°$)		GPS only	GPS+QZSS1	GPS+QZSS2	GPS+QZSS3
Whole Area	NVS ≥ 4	84.23%	95.85%	88.57%	96.96%
Positioning Available Area ($\mathrm{NVS}_{\mathtt{All}} \geq 4$)	MIN	2.63	2.42	2.37	2.43
	MEAN	10.13	8.04	8.18	7.32
	MAX	536.76	81.97	295.36	315.42

5.3.1 Spatial Variations of ASR

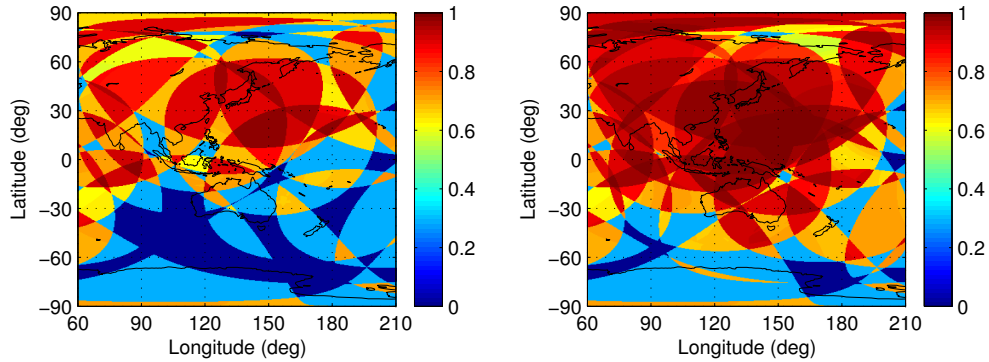

(a) GPS Only

(b) GPS and QZSS Option 1

(c) GPS and QZSS Option 2

(d) GPS and QZSS Option 3

System ($30°$)		GPS only	GPS+QZSS1	GPS+QZSS2	GPS+QZSS3
Whole Area	NVS ≥ 4	84.23%	95.85%	88.57%	96.96%
Positioning Available Area ($NVS_{All} \geq 4$)	MIN	28.93%	28.93%	28.93%	28.93%
	MEAN	60.72%	79.75%	77.19%	81.04%
	MAX	98.75%	99.64%	99.66%	99.64%

5.3.1 Spatial Variations of MDB

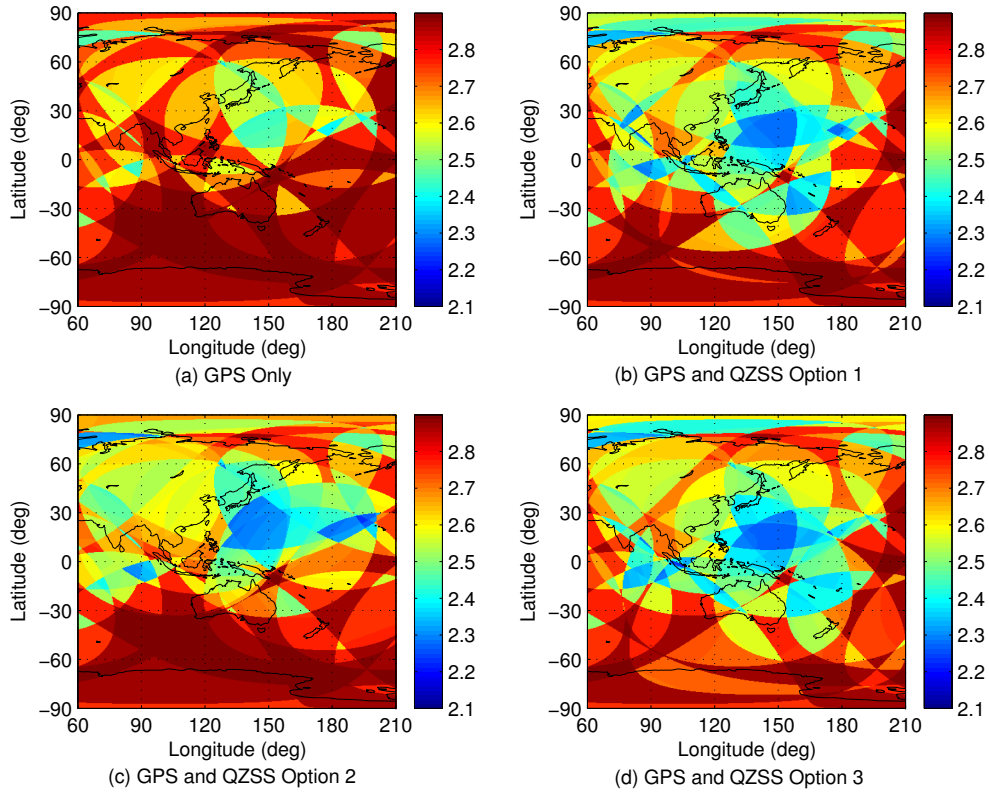

(a) GPS Only

(b) GPS and QZSS Option 1

(c) GPS and QZSS Option 2

(d) GPS and QZSS Option 3

System ($30°$)		GPS only	GPS+QZSS1	GPS+QZSS2	GPS+QZSS3
Whole Area	NVS ≥ 4	84.23%	95.85%	88.57%	96.96%
Positioning Available Area ($NVS_{All} \geq 4$)	MIN	2.38	2.17	2.23	2.15
	MEAN	2.74	2.62	2.64	2.60
	MAX	2.86	2.86	2.86	2.86

5.3.1 Spatial Variations of MDE

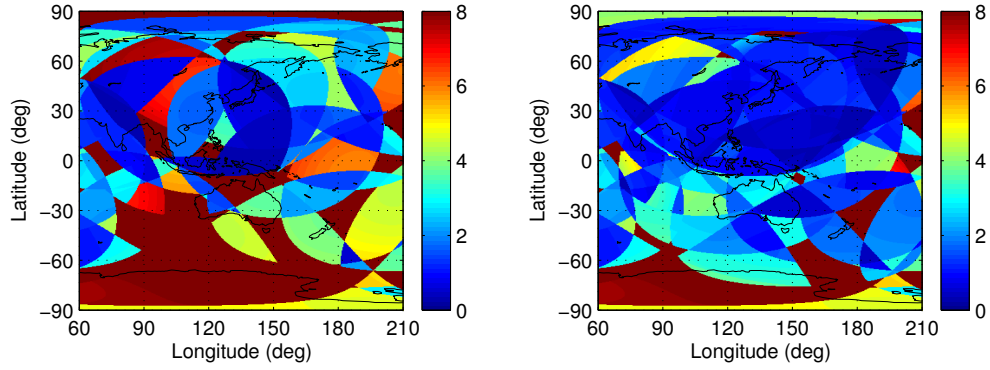

(a) GPS Only

(b) GPS and QZSS Option 1

(c) GPS and QZSS Option 2

(d) GPS and QZSS Option 3

System ($30°$)		GPS only	GPS+QZSS1	GPS+QZSS2	GPS+QZSS3
Whole Area	NVS ≥ 4	84.23%	95.85%	88.57%	96.96%
Positioning	MIN	0.27	0.21	0.23	0.25
Available Area	MEAN	4.55	2.35	2.68	2.37
($\mathrm{NVS}_{\mathtt{All}} \geq 4$)	MAX	278.07	24.93	260.02	276.87

5.3.1 Summary of Spatial Variations

System (Elevation Mask: $30°$)			GPS Only	GPS + QZSS 1	GPS + QZSS 2	GPS + QZSS 3
Whole Area	NVS ≥ 4		84.23%	95.85%	88.57%	96.96%
Positioning Available Area ($NVS_{All} \geq 4$)	NVS	MAX	8	10	11	10
		MEAN	5.00	6.16	6.20	6.15
	GDOP	MIN	2.63	2.42	2.37	2.43
		MEAN	10.13	8.04	8.18	7.32
	ASR	MAX	98.75%	99.64%	99.66%	99.64%
		MEAN	60.72%	79.75%	77.19%	81.04%
	MDB	MIN	2.38	2.17	2.23	2.15
		MEAN	2.74	2.62	2.64	2.60
	BNR	MIN	3.14	2.54	2.74	2.48
		MEAN	3.97	3.78	3.84	3.75
	MDE	MIN	0.27	0.21	0.23	0.25
		MEAN	4.55	2.35	2.68	2.37

5.3.2 Temporal Variations of NVS

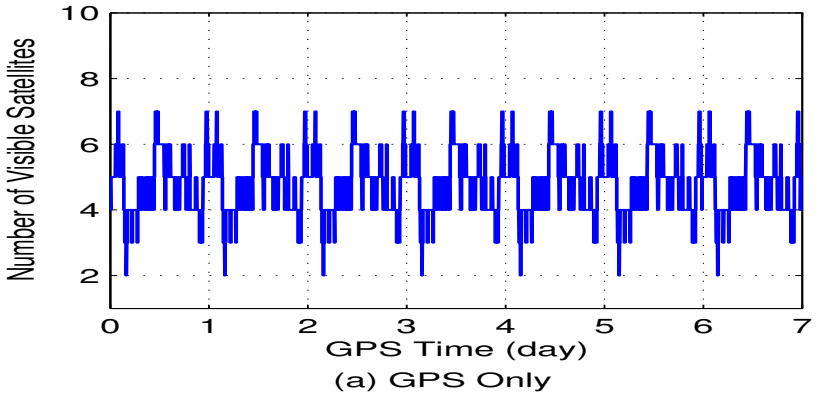

(a) GPS Only

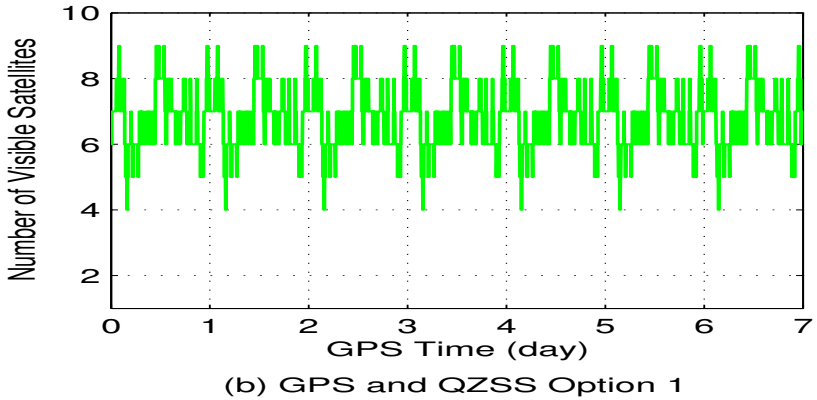

(b) GPS and QZSS Option 1

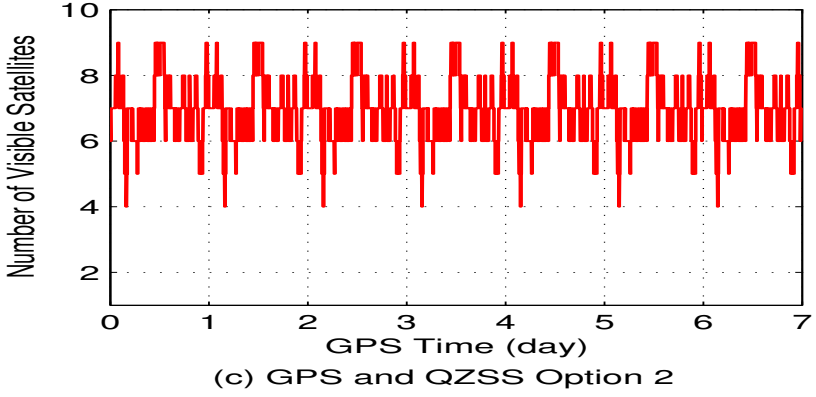

(c) GPS and QZSS Option 2

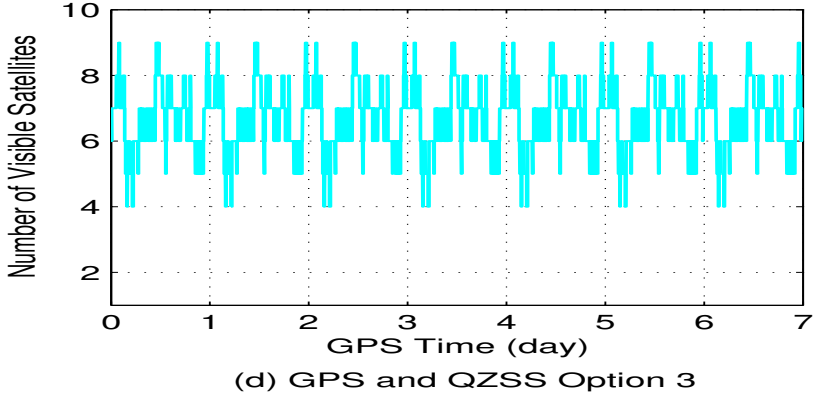

(d) GPS and QZSS Option 3

System (Tokyo, $30°$)		GPS only	GPS+QZSS1	GPS+QZSS2	GPS+QZSS3
Whole Time	NVS ≥ 4	94.43%	100.00%	100.00%	100.00%
Positioning	MIN	4	6	6	5
Available Time	MEAN	4.88	6.89	7.05	6.78
($\mathrm{NVS}_{\mathtt{All}} \geq 4$)	MAX	7	9	9	9

5.3.2 Temporal Variations of GDOP

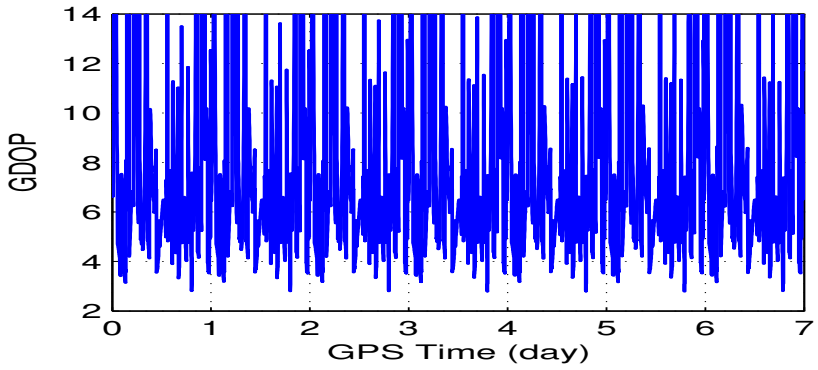

(a) GPS Only

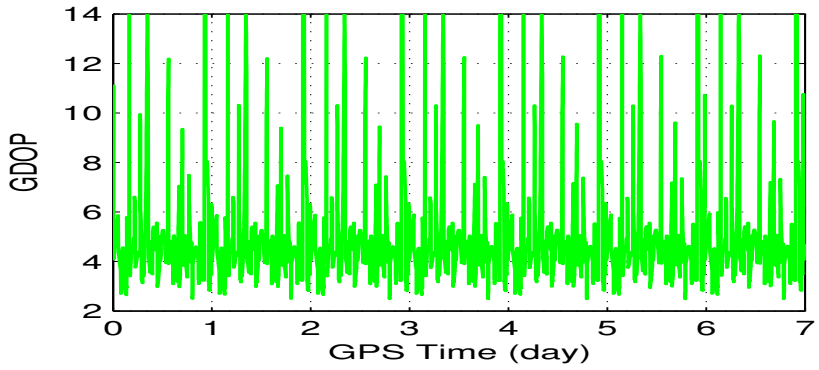

(b) GPS and QZSS Option 1

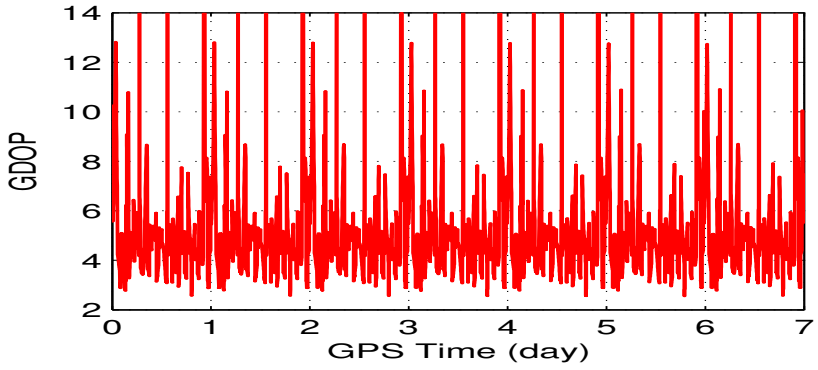

(c) GPS and QZSS Option 2

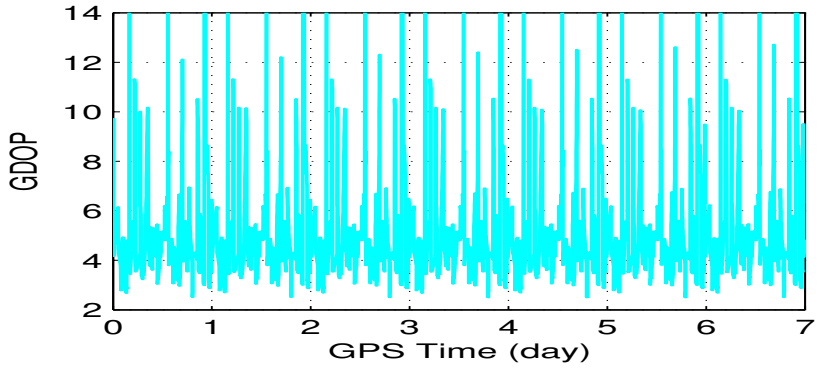

(d) GPS and QZSS Option 3

System (Tokyo, $30°$)		GPS only	GPS+QZSS1	GPS+QZSS2	GPS+QZSS3
Whole Time	NVS ≥ 4	94.43%	100.00%	100.00%	100.00%
Positioning	MIN	2.78	2.47	2.55	2.50
Available Time	MEAN	16.37	4.80	5.20	4.93
($\mathrm{NVS}_{\mathtt{All}} \geq 4$)	MAX	4892.42	20.24	58.63	24.76

5.3.2 Temporal Variations of ASR

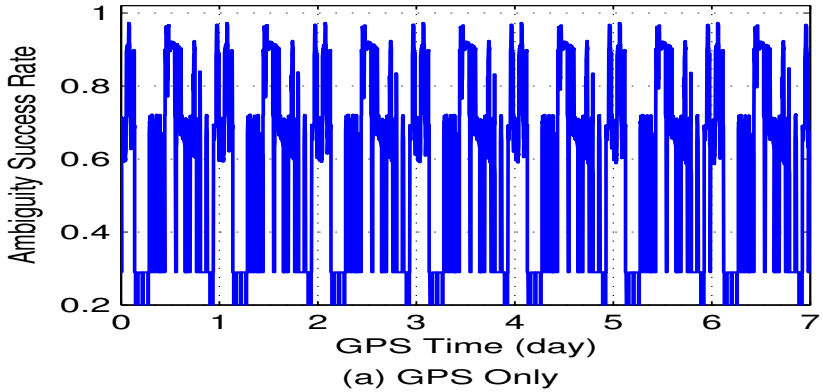

(a) GPS Only

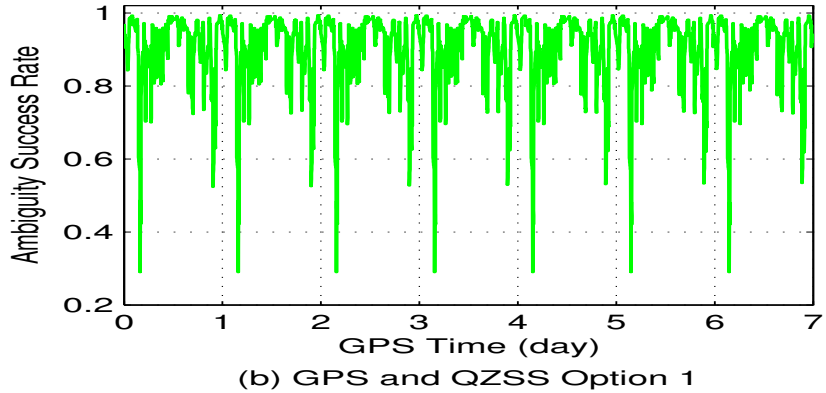

(b) GPS and QZSS Option 1

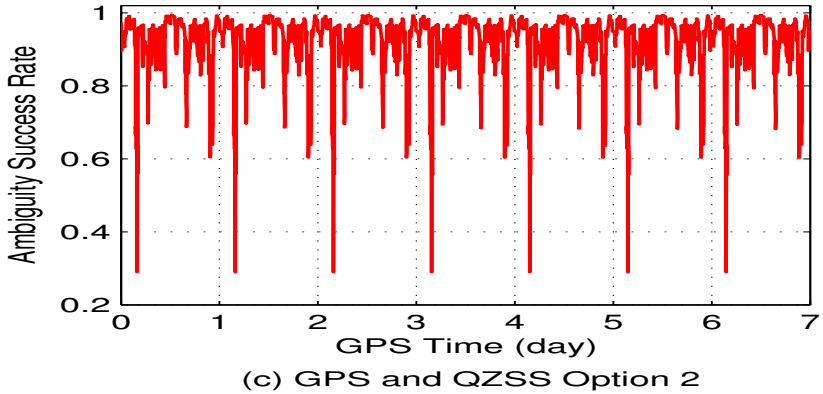

(c) GPS and QZSS Option 2

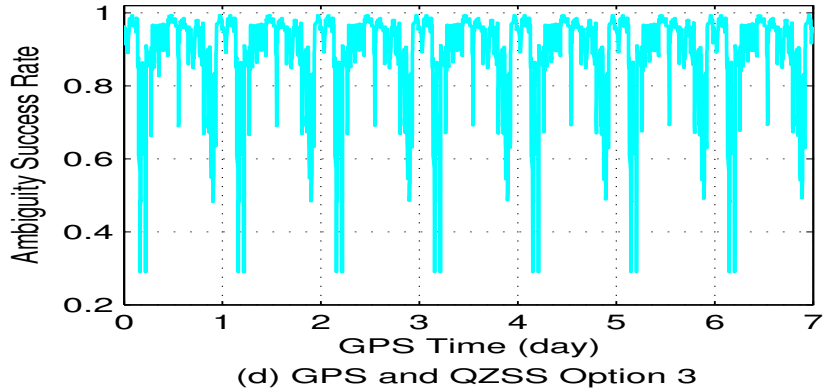

(d) GPS and QZSS Option 3

System (Tokyo, $30°$)		GPS only	GPS+QZSS1	GPS+QZSS2	GPS+QZSS3
Whole Time	NVS ≥ 4	94.43%	100.00%	100.00%	100.00%
Positioning	MIN	28.93%	72.29%	68.14%	53.97%
Available Time	MEAN	57.94%	92.18%	93.76%	91.40%
($\mathrm{NVS}_{\mathtt{All}} \geq 4$)	MAX	97.35%	99.45%	99.39%	99.44%

5.3.2 Temporal Variations of MDB

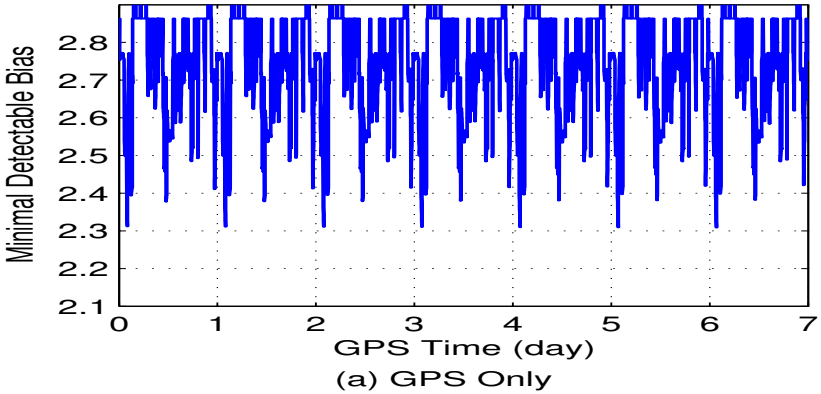

(a) GPS Only

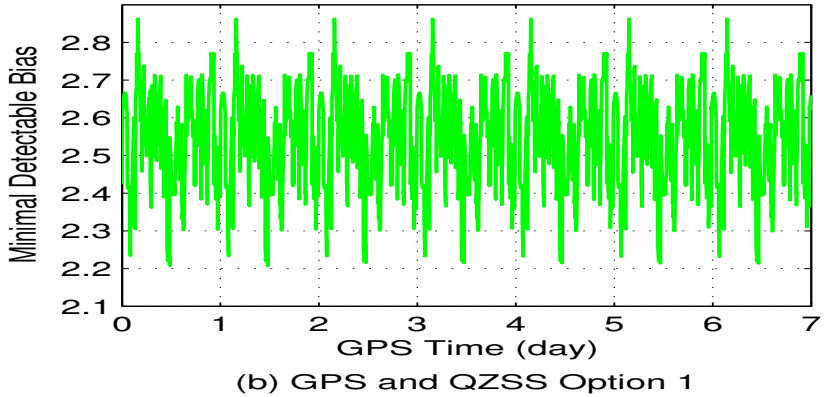

(b) GPS and QZSS Option 1

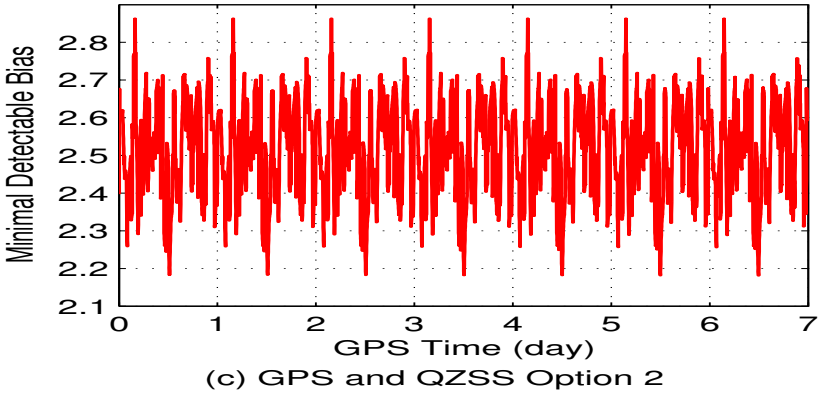

(c) GPS and QZSS Option 2

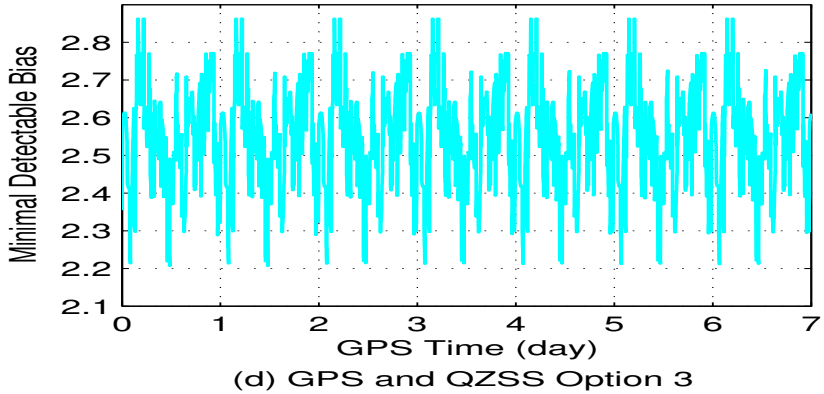

(d) GPS and QZSS Option 3

System (Tokyo, $30°$)		GPS only	GPS+QZSS1	GPS+QZSS2	GPS+QZSS3
Whole Time	NVS ≥ 4	94.43%	100.00%	100.00%	100.00%
Positioning	MIN	2.31	2.21	2.18	2.20
Available Time	MEAN	2.74	2.53	2.51	2.53
($\mathrm{NVS}_{\mathtt{All}} \geq 4$)	MAX	2.86	2.72	2.72	2.77

5.3.2 Temporal Variations of MDE

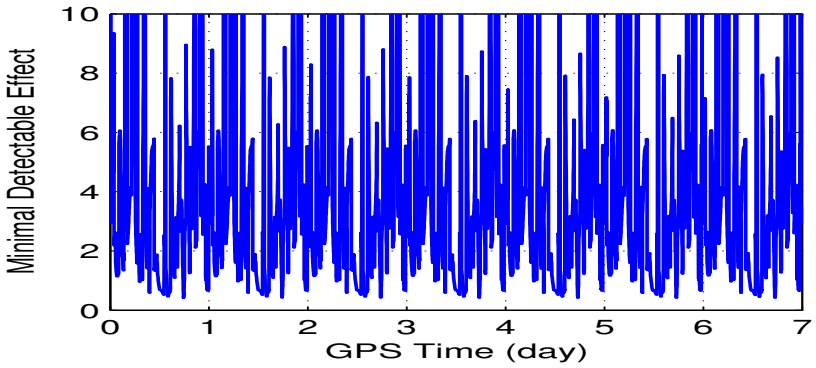

(a) GPS Only

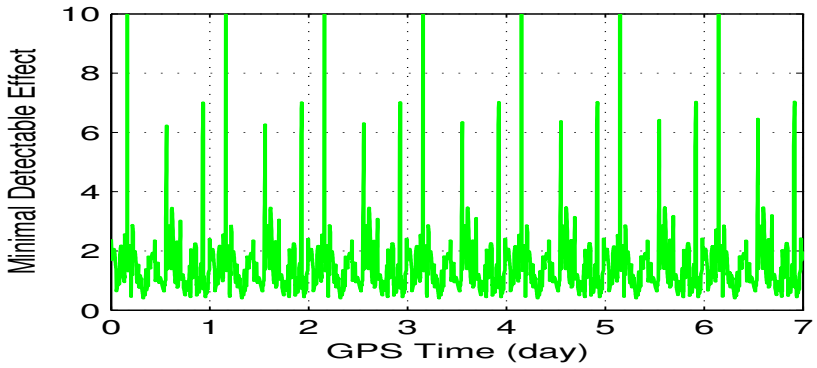

(b) GPS and QZSS Option 1

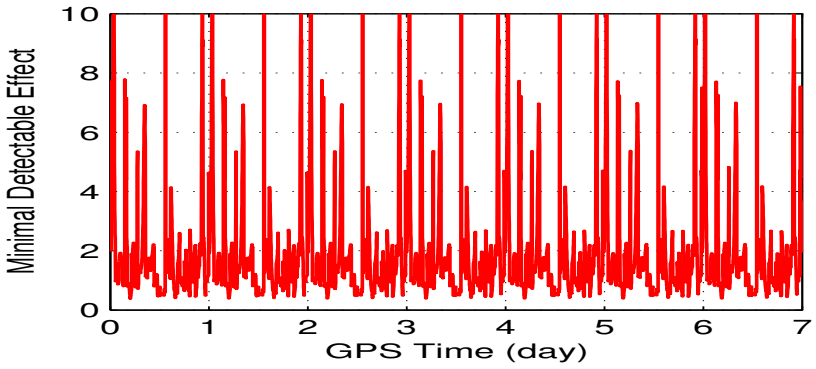

(c) GPS and QZSS Option 2

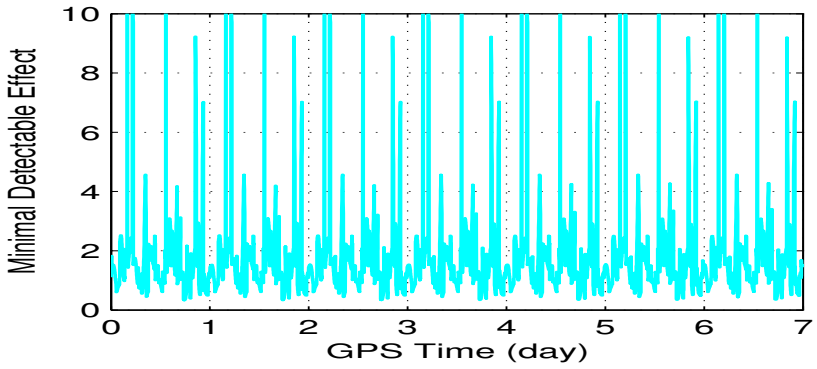

(d) GPS and QZSS Option 3

System (Tokyo, $30°$)		GPS only	GPS+QZSS1	GPS+QZSS2	GPS+QZSS3
Whole Time	NVS ≥ 4	94.43%	100.00%	100.00%	100.00%
Positioning	MIN	0.41	0.39	0.38	0.33
Available Time	MEAN	9.57	1.39	1.85	1.61
($\mathrm{NVS}_{\mathtt{All}} \geq 4$)	MAX	3546.50	6.46	48.73	16.21

5.3.2 Summary of Temporal Variations

System (Tokyo) (Elevation Mask: $30°$)			GPS Only	GPS + QZSS 1	GPS + QZSS 2	GPS + QZSS 3
Whole Time	NVS ≥ 4		94.43%	100.00%	100.00%	100.00%
Positioning Available Time ($NVS_{All} \geq 4$)	NVS	MAX	7	9	9	9
		MEAN	4.88	6.89	7.05	6.78
	GDOP	MIN	2.78	2.47	2.55	2.50
		MEAN	16.34	4.80	5.20	4.93
	ASR	MAX	97.35%	99.45%	99.39%	99.44%
		MEAN	57.94%	92.18%	93.76%	91.40%
	MDB	MIN	2.31	2.21	2.18	2.20
		MEAN	2.74	2.53	2.51	2.53
	BNR	MIN	2.87	2.62	2.52	2.63
		MEAN	3.95	3.63	3.57	3.61
	MDE	MIN	0.41	0.39	0.38	0.33
		MEAN	9.55	1.39	1.85	1.61

5.4 Summary

- GPS augmentation using Japanese QZSS have been analyzed.
- Three QZSS satellite constellation options have been investigated, and the achievable performances are obtained by software simulation.
- QZSS will not only improve the satellite visibility, and extend the positioning available time and area, and offer better GDOP, but also enhances the capability of carrier phase based positioning in Japan and its neighboring areas.
- The first QZSS option (Asymmetrical 8-shape) is the best option for Japan, although the third QZSS option (Symmetrical 8-shape) is the best option for the whole Asian-Pacific, Australian area.

6. Development of a Prototype SGR

- Software GPS/GNSS Receiver
- GPS C/A Code Acquisition
  - Conventional approach
  - FFT approach
- GPS Signal Tracking
  - Code Tracking
  - Carrier Tracking
- Summary

6.1 Background

- New Satellite Navigation Signals
  - Modernized GPS (USA);
  - Galileo (EU);
  - Japanese Quasi-Zenith Satellite System (QZSS).
- New Positioning Applications
  - E911 call service for wireless phones (US), E110 (Japan, Newspaper Asahi, Nov.6, 2003);
  - Hardware size and power consumption of GPS receiver.
- Software GPS/GNSS receiver: the signal acquisition and tracking are implemented by software instead of hardware chip.

6.2 Software GPS/GNSS Receiver

- Four Classes
  (1) PC based genuine software GPS/GNSS receiver;
  (2) Digital Signal Processors (DSP) based software GPS/GNSS receiver;
  (3) Field Programmable Gate Array (FPGA) based software GPS/GNSS receiver;
  (4) Simulation tools.
- Two Groups
  (1) Radio Frequency (RF) sampling;
  (2) Intermediate Frequency (IF) sampling.
- A prototype PC based and IF sampling software GPS receiver has been developed.

6.2 General Structure of SGR

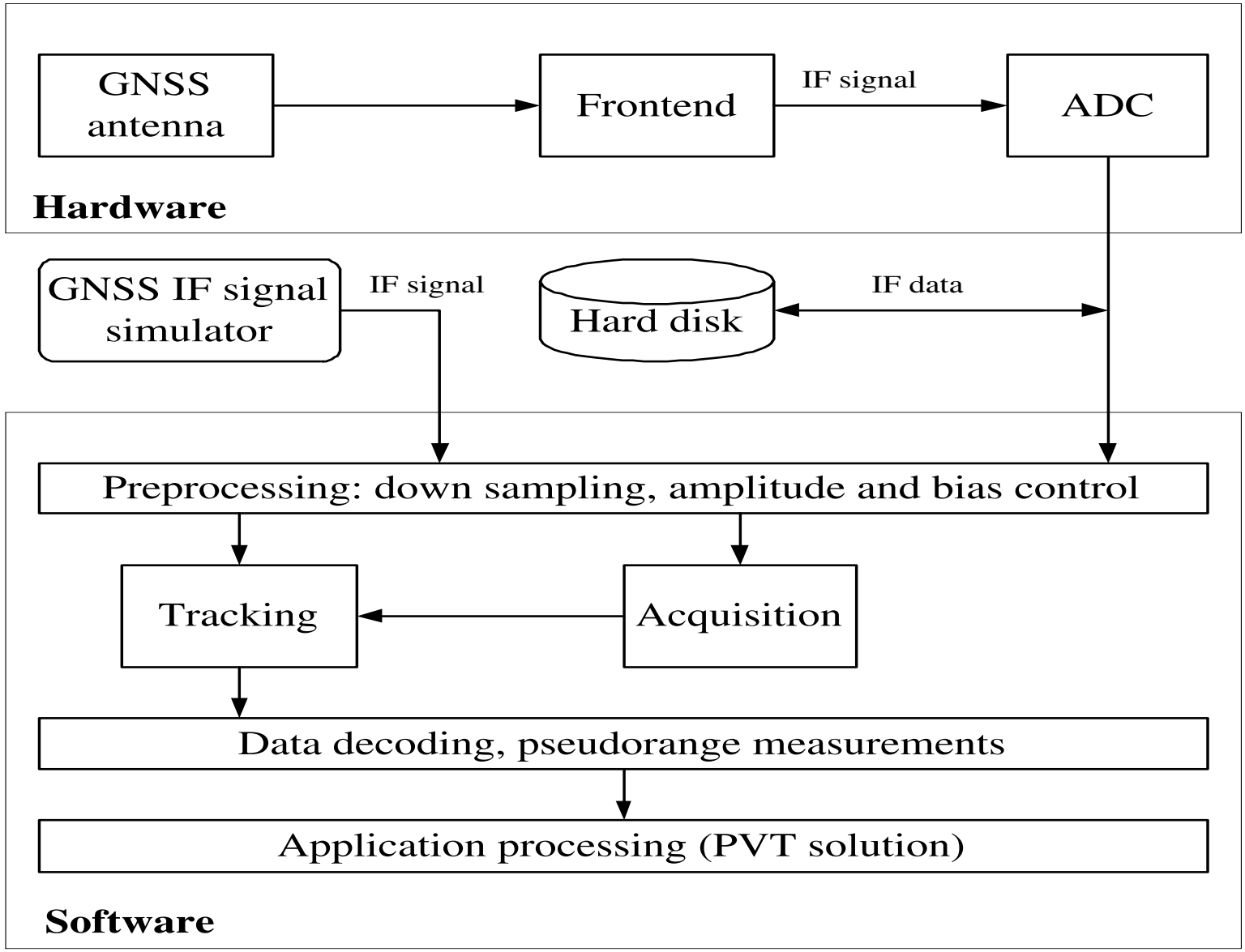

6.3.2 Acquisition (Conventional)

- Non coherent correlator in time domain

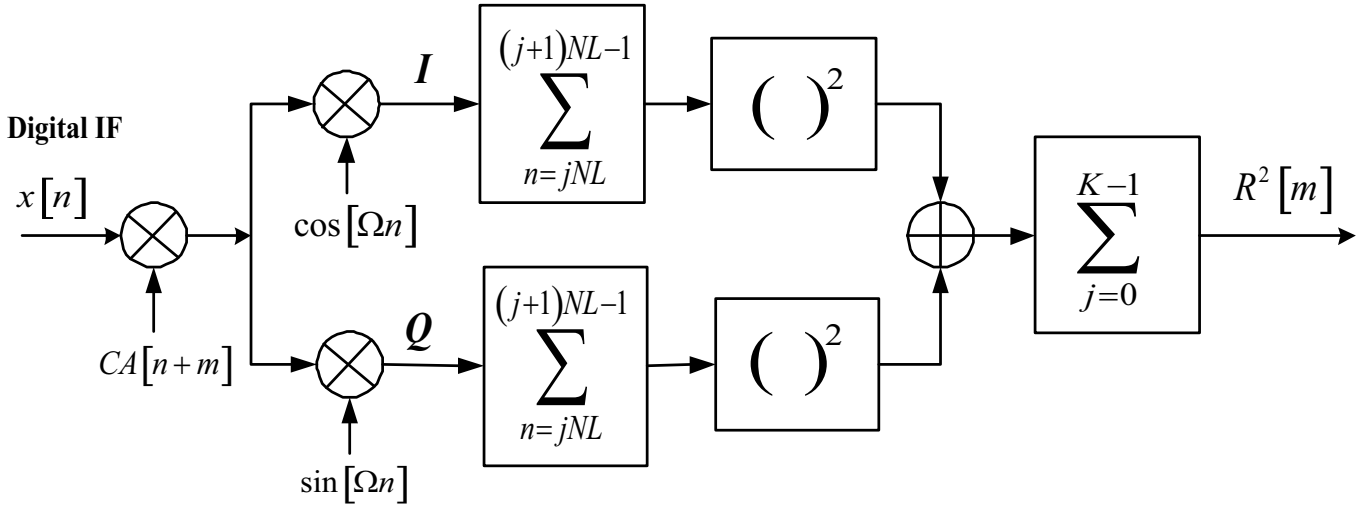

- Correlation Power

$$R^2[m] = \sum_{j=0}^{K-1} \left(\left[\sum_{n=jNL}^{(j+1)NL-1} x[n] \cdot CA[n] \cdot \cos[\Omega n] \right]^2 + \left[\sum_{n=jNL}^{(j+1)NL-1} x[n] \cdot CA[n] \cdot \sin[\Omega n] \right]^2 \right)$$

6.3.2 Acquisition (FFT)

- Conventional approach can also be performed in circular convolution

$$R[m] = \sum_{n=0}^{L-1} x[n] \cdot CA[((n+m))_L]$$

- Non coherent correlator in frequency domain

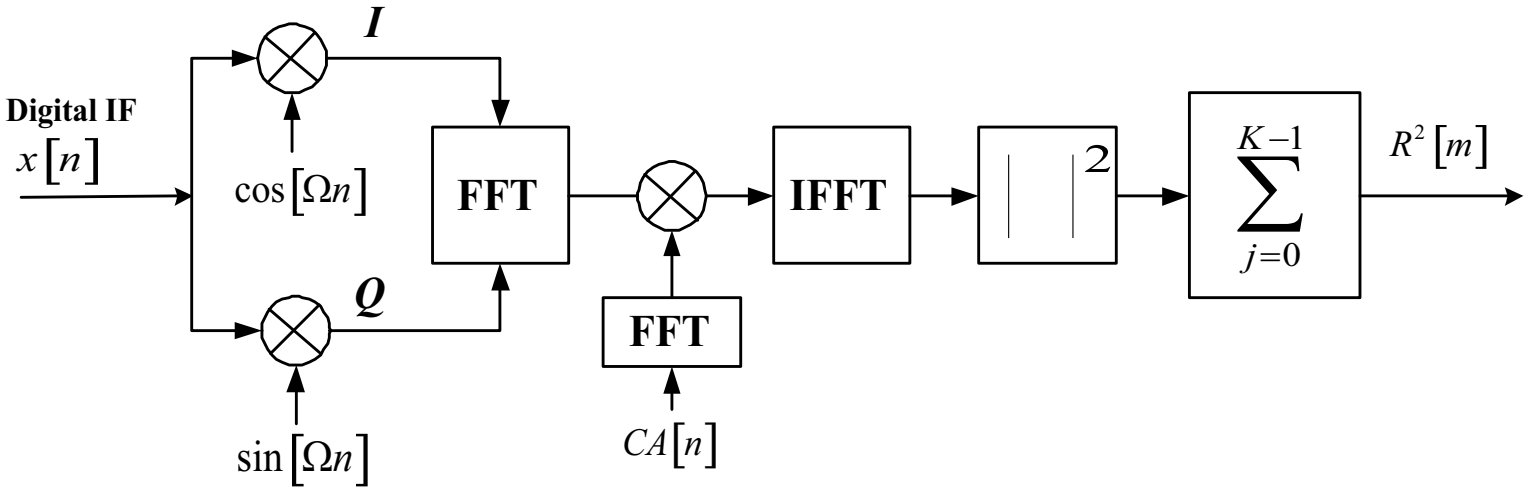

$$R[m] = \underbrace{x[n] \otimes CA[-n]}_{Circular\ convolution} = F^{-1}\left(F(x[n]) \cdot F(CA[n])^*\right)$$

6.3.2 Acquisition Results (FFT)

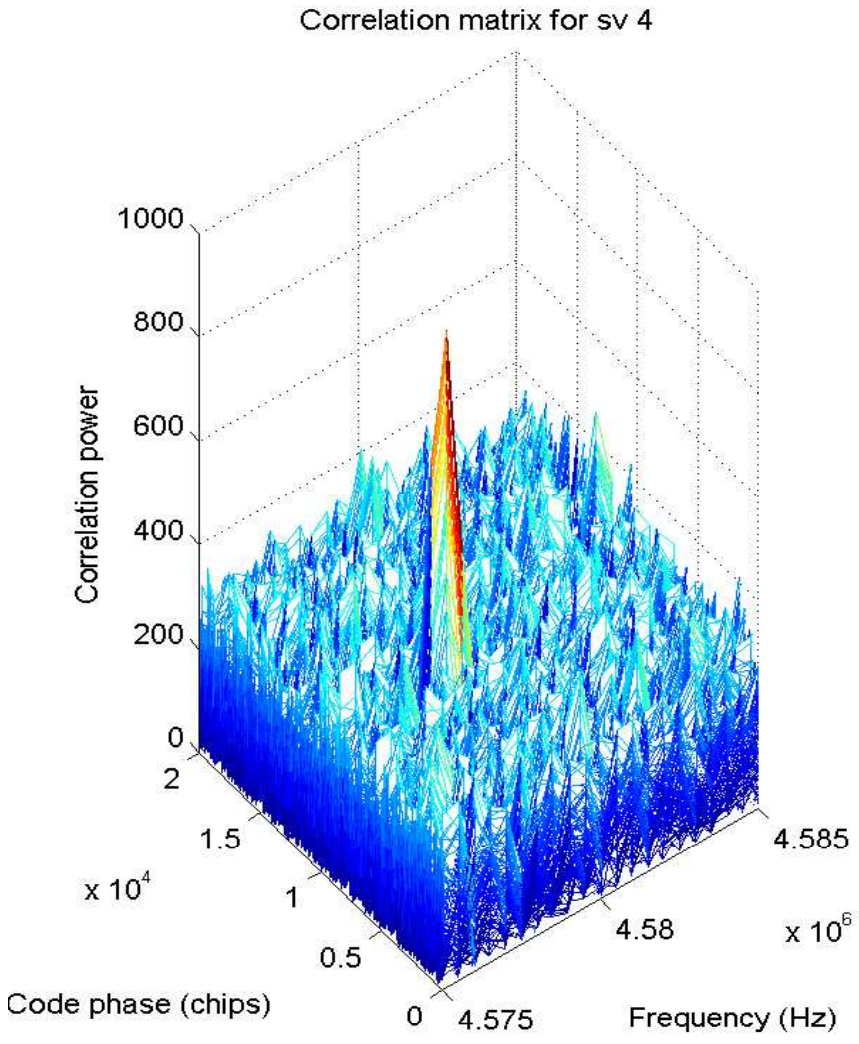

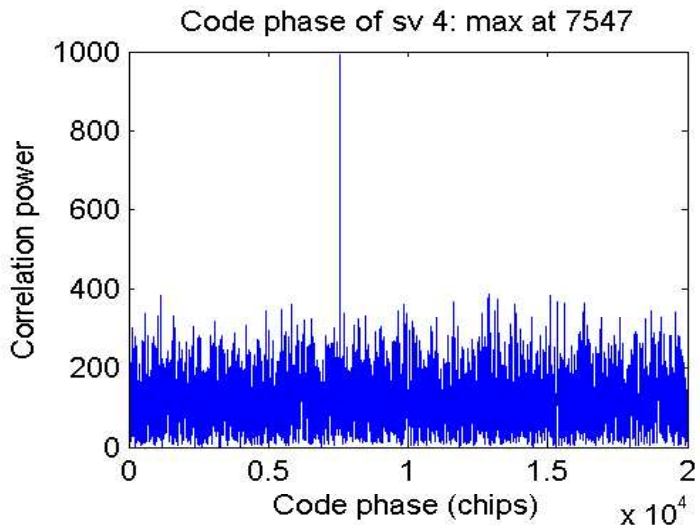

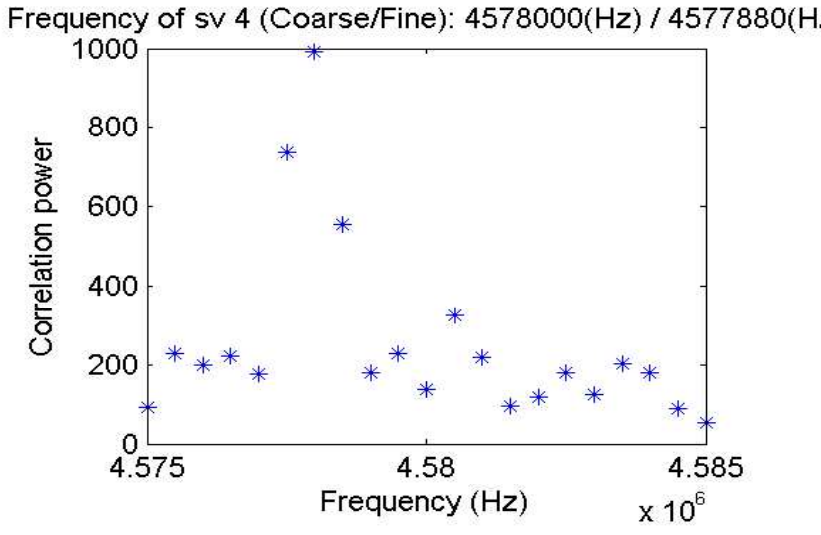

6.4 GPS Signal Tracking

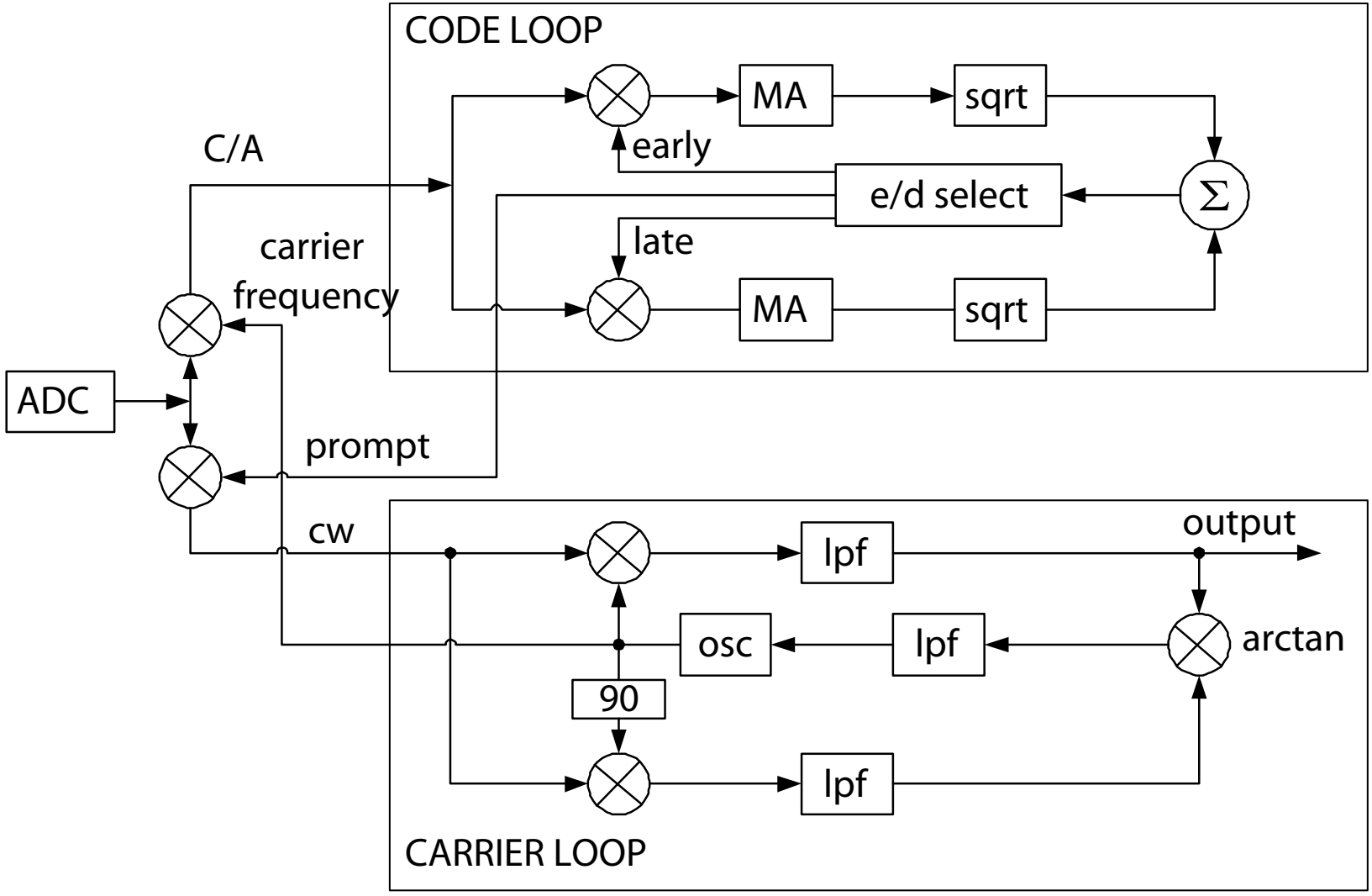

6.4.1 Code Tracking

- Delay Lock Loop (DLL)

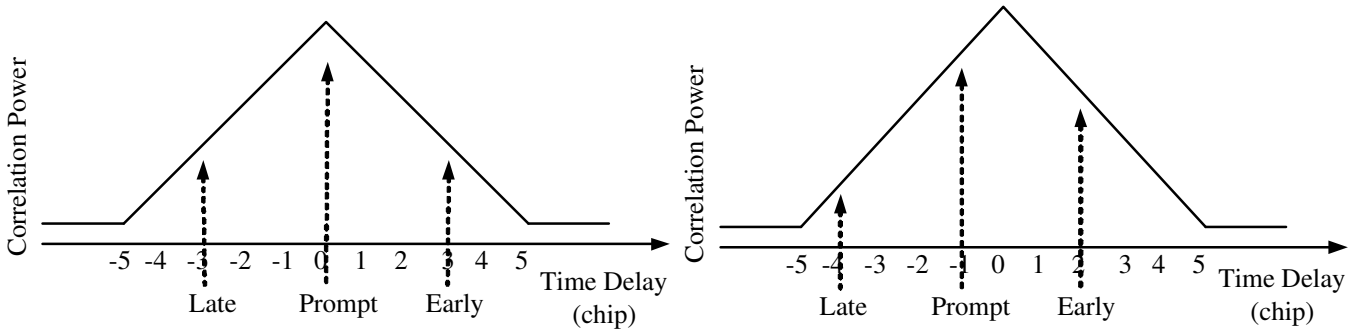

(a) Correlation without phase error

(b) Correlation with phase error

- The discriminator output signal, $\varepsilon = \frac{y_E}{y_L}$
  - if $\varepsilon = 1$, the prompt code is perfectly aligned with the C/A code in the input signal;
  - if $\varepsilon > 1.5$, the local codes should be shifted to the right;
  - if $\varepsilon < 0.8$, the local codes should be shifted to the left.

6.4.1 Code Tracking

- Correlation power of early, prompt and late channel

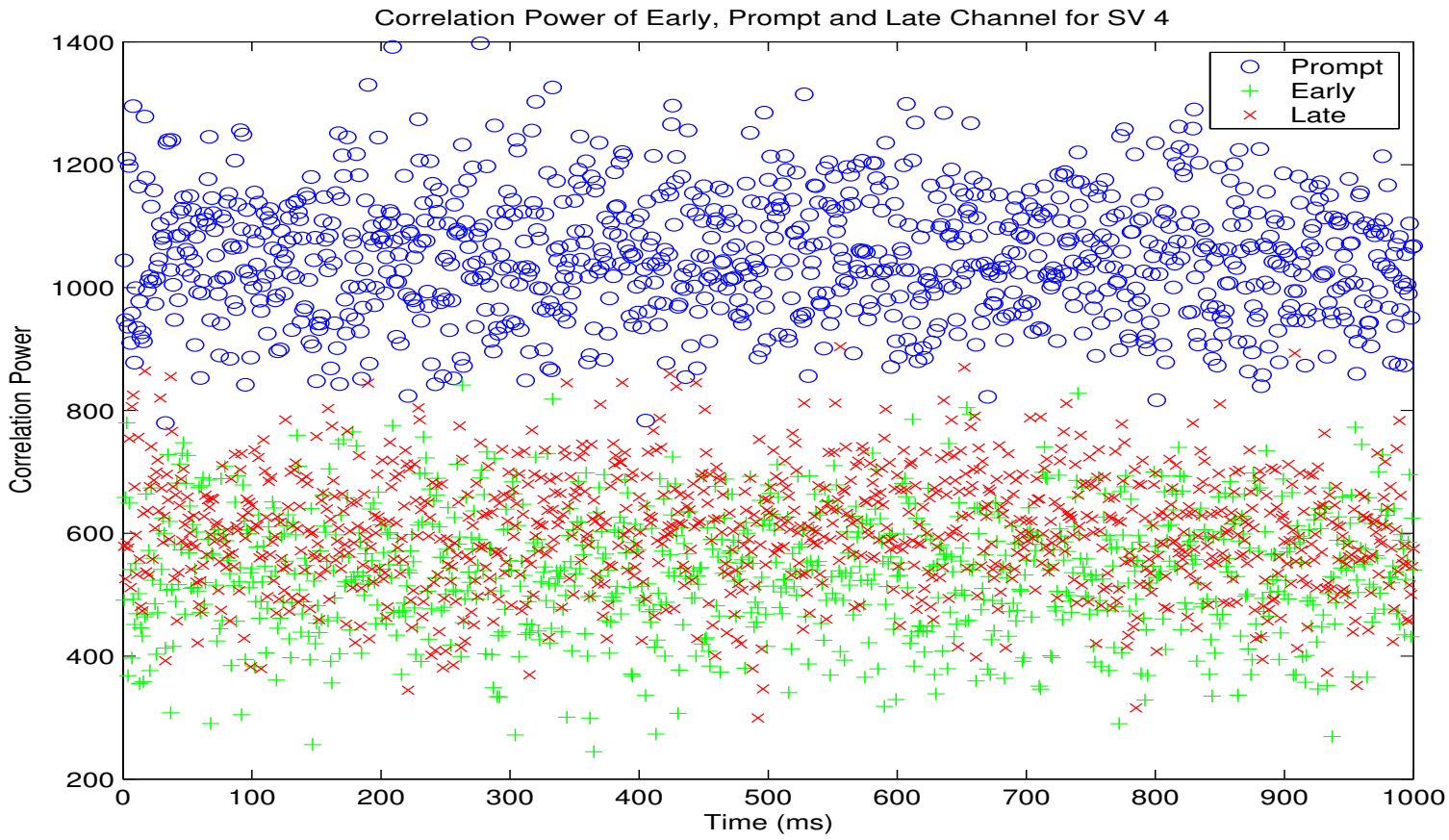

- Code tracking loop keeps the prompt signal at maximum correlation.

6.4.2 Carrier Tracking

- Carrier Tracking Loop

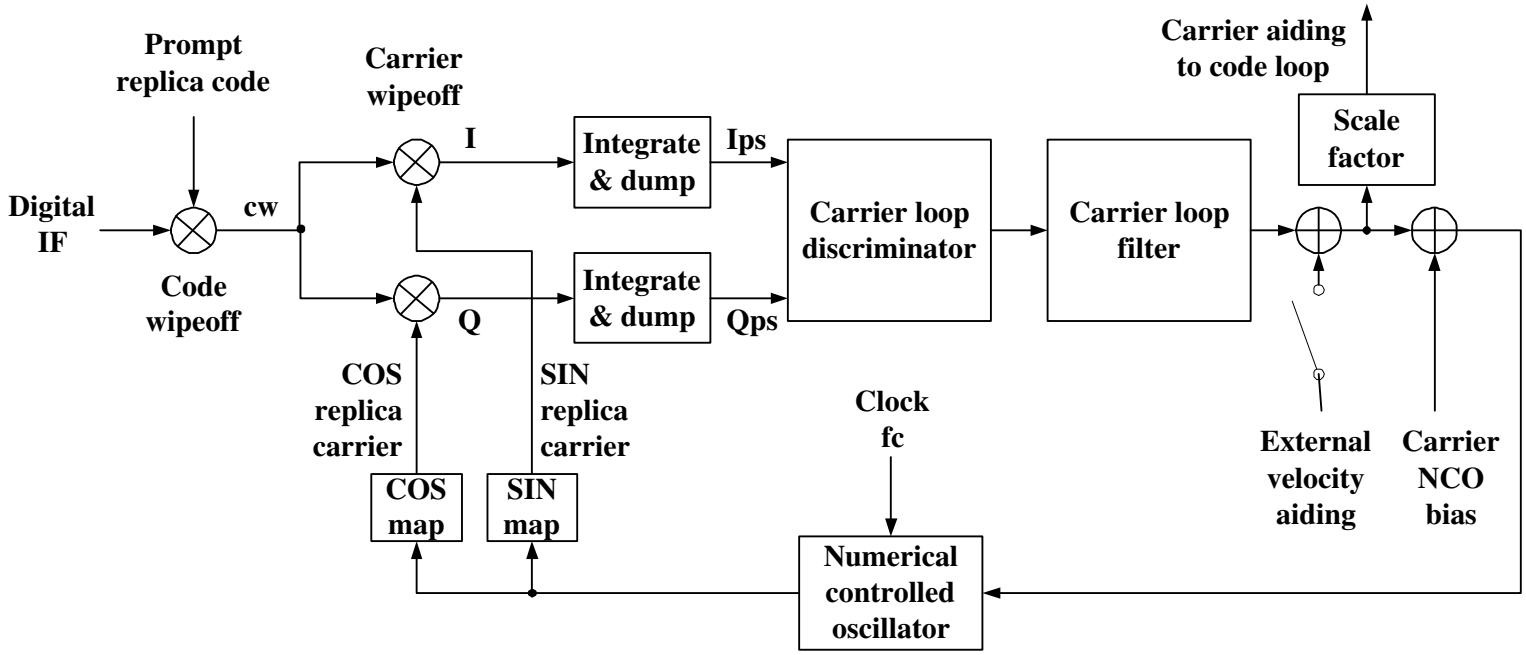

- $\theta_{corr} = remainder\left(\theta_{old} + \theta, 2\pi\right)$
- Carrier Loop Filter (Second-order Filter)

$$F\left(z\right) = \frac{\left(C_1 + C_2\right) - C_1 * z^{-1}}{1 - z^{-1}}$$

6.4.2 Carrier Tracking

- Outputs from carrier tracking loop

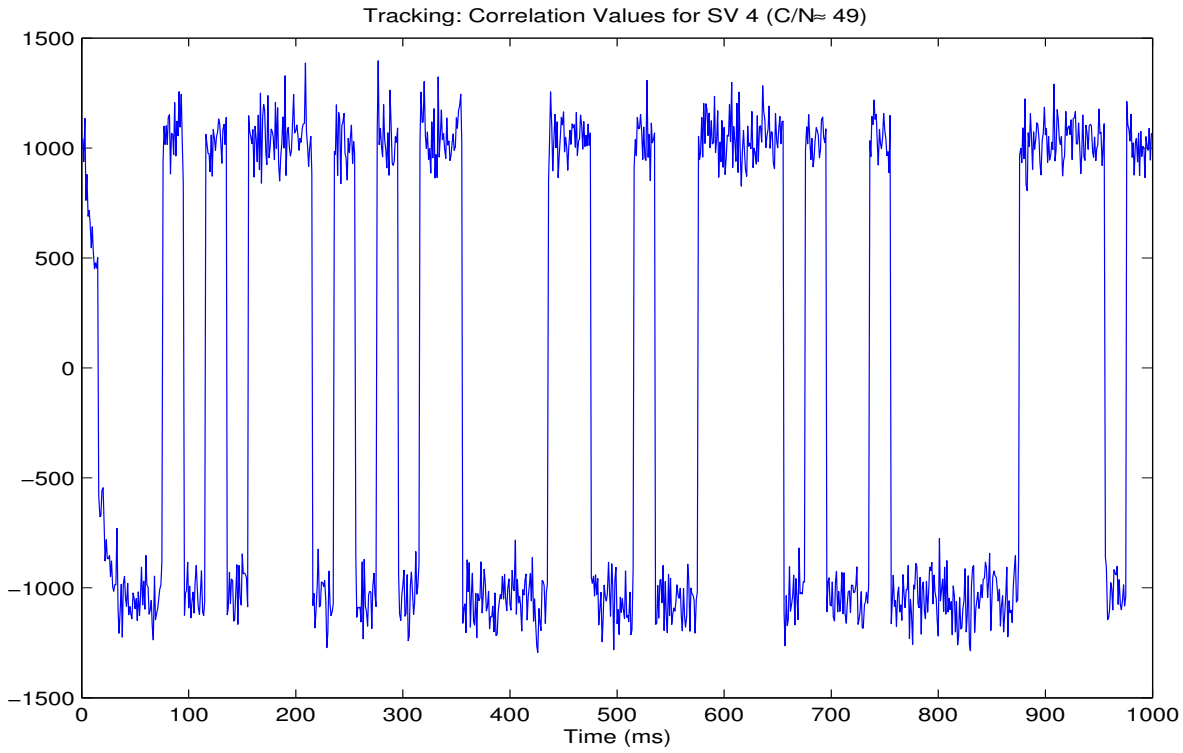

- Navigation Data Phase Transition $\Rightarrow$ Navigation Data $\Rightarrow$ Ephemeris data and pseudorange $\Rightarrow$ PVT

6.5 Summary

- A prototype PC based and IF sampling software GPS receiver;
- Two acquisition methods
  - Conventional approach;
  - FFT approach.
- The code and carrier tracking methods have been investigated.

Contents

7.1 Conclusions

- An approach for GPS carrier phase ambiguity resolution using altitude-aiding has been proposed;
- A method using MRS for estimating the distance-dependant delays has been developed;
- The performance of hybrid modernized GPS and Galileo positioning and navigation has been analyzed;
- The performance of the GPS augmentation using QZSS has been evaluated;
- A prototype software GPS receiver has been developed.

7.2 Recommendations

- Hybrid Modernized GPS and Galileo Positioning and Navigation
  - To study high precision positioning using linear combination signals of hybrid modernized GPS and Galileo;
  - To analyze the performance of GNSS global and regional integrity.
- GPS Augmentation Using Japanese QZSS
  - To design the signal structure of QZSS;
  - To investigate the integrity and continuity of GPS augmentation using QZSS.

7.2 Recommendations

- Software GNSS/SBAS Receiver
  - To develop a GNSS/SBAS signal processing algorithm for GNSS/SBAS receivers;
  - To design a RF front-end for the reception of multi-frequency signals from GNSS/SBAS
  - To mitigate the multipath on GNSS/SBAS receivers;
  - To develop a method for performs GNSS/SBAS Signal Quality Monitoring (SQM).

Acknowledgements

- To Professor *Akio Yasuda*, my principal supervisor!
- To Professor *Masaki Oshima*, my second supervisor!
- To Professor *Hideki Hagiwara* and Dr. *Sakae Nagaoka*, the members of my examining committee!
- To Professor *Harumasa Hojo*, Mr. *Nobuaki Kubo* and Mr. *Masashi Kawamura*!
- To Mr. *Peter Joosten* and Ms. *Sandra Verhagen*!
- To may current and former colleagues at the Laboratory of Communications Engineering of TUMST!
- To my parents and my wife!

Thank you for your attention!

fwu@e.kaiyodai.ac.jp
Laboratory of Communication Engineering,
Tokyo University of Marine Science and Technology